



Residential Heat Pump Efficiency Rating Representativeness Project

PHASE 1

OCTOBER 2024



Table of Contents

Acknowledgements	4
Section 1: Introduction	5
1.1 Study objectives.....	6
1.2 Research questions.....	6
1.3 Study overview	7
Section 2: MEASUREMENT AND VERIFICATION ACTIVITIES	9
2.1 Test site description.....	9
2.2 Mobile home infiltration, conduction, and capacitance	10
2.2.1 Infiltration test.....	11
2.2.2 Co-heating (conduction) tests.....	12
2.2.3 Capacitance tests.....	15
2.3 Heat pump installation and ductwork	21
2.3.1 House 1.....	23
2.3.2 House 2.....	25
2.3.3 House 3.....	27
2.4 Instrumentation installation	29
2.4.1 Power.....	32
2.4.2 Airflow	33
2.4.3 Air temperature and humidity.....	34
2.4.4 Refrigerant measurements	38
2.4.5 Internal gains	40
2.4.6 Weather station	42
2.5 Conduct tests.....	43
2.5.1 Cooling.....	45
2.5.2 Heating	47
2.6 Heat pump decommissioning	48
2.7 Data dashboard	50
2.7.1 Direct measurements	50
2.7.2 Calculated measurements	52
Phase 2: (LAB TESTING) AND NEXT STEPS	63



List of Figures

Figure 1-1. Daily temperature, high and low, in °F	7
Figure 2-1. Map of mobile home community in Lincoln, NE – selected homes circled in red	9
Figure 2-2. CSA SPE-07 heating load line as a function of outdoor air temperature	13
Figure 2-3. House 1 – north-facing window – lower sash replaced with sheet metal	14
Figure 2-5. Close up of lower window sash replaced with steel sheet metal	14
Figure 2-4. House 1 – three south-facing windows – lower sashes replaced with sheet metal	14
Figure 2-6. House 2 – Section of supply ductwork exposed to increase conductance	14
Figure 2-7. Heating load lines for all houses, calibration period	15
Figure 2-8. Example of heater cycles and deadband for Houses 1, 2, and 3 (top to bottom)	17
Figure 2-9. Scatter plot of N vs. X (1-X) for each house	18
Figure 2-10. Drywall sheets installed in living room area to increase shallow thermal mass	20
Figure 2-11. Drywall sheets installed in “bedroom 1”	20
Figure 2-12. Ducted HP ductwork ends in utility room facing native furnace return	22
Figure 2-13. System A bent hail guard	23
Figure 2-14. Broken latch on filter case	23
Figure 2-15. System A bent and damaged fins	23
Figure 2-16. System A outdoor unit	24
Figure 2-18. System A indoor unit, showing duct	24
Figure 2-17. System A indoor unit with mass flow sensor	24
Figure 2-19. System D outdoor unit	25
Figure 2-20. System D indoor unit with mass flow sensors	25
Figure 2-21. House 2 – outdoor units and exposed underbelly	26
Figure 2-22. System B outdoor unit	26
Figure 2-24. System B indoor let set and mass flow sensor (not shown at bottom)	26
Figure 2-23. System B indoor unit	26
Figure 2-25. System E outdoor unit	27
Figure 2-27. System C outdoor unit	27
Figure 2-26. System E indoor unit with mass flow sensor	27
Figure 2-28. System C indoor unit and duct	27
Figure 2-29. System C indoor unit line set and mass flow sensor	28
Figure 2-30. System F fin and tube damage	28
Figure 2-31. System F fin damage	28
Figure 2-32. System F indoor unit and mass flow sensor	29
Figure 2-33. System F outdoor unit	29
Figure 2-34. System F ODU with shrouds removed, thermocouples and pressure gauges installed	29
Figure 2-35. House electrical panel and CTs	32
Figure 2-36. Two CTs (one rated 1A and one rated 5A) measuring indoor unit power	32
Figure 2-37. Ducted HP flow plate in filter slot (system A and B)	33
Figure 2-38. System C flow plate position (filter cover removed to show plate)	33
Figure 2-39. System D temperature and RH sensor arrays	35
Figure 2-40. System D return/inlet temperature/RH sensors	35
Figure 2-41. System C supply air plenum thermocouple array	35
Figure 2-42. Ductless HP supply/outlet air temperature/RH sensors	36
Figure 2-43. Ducted HP inlet air temperature sensor location	36
Figure 2-44. “Thermostat” thermocouple	36
Figure 2-45. “BR2” wireless temperature and humidity sensor	36
Figure 2-46. System F outlet T/RH sensors 1 through 4	37
Figure 2-47. System F outlet T/RH sensors 1 through 4 readings	37



Figure 2-48. House 1 ductless HP refrigerant mass flow sensors	38
Figure 2-49. House 1 ducted HP refrigerant mass flow sensor	39
Figure 2-50. Ductless HP, pressure gauge T-tap	39
Figure 2-51. Ductless HP thermocouple, true suction	39
Figure 2-52. House 2 ducted HP refrigerant mass flow sensor and gauge pressure sensors	39
Figure 2-53. Daily latent load shape	40
Figure 2-54. Weather station located at House 1	42
Figure 2-55. House 2 underbelly water leak due to pipe freeze and rupture	48
Figure 2-56. Probe location for inlet and discharge, system A	49
Figure 2-57. Probe location for inlet, system A	49
Figure 2-58. System B pressure gauge drift	51

List of Tables

Table 2-1. Study calibration metrics	10
Table 2-2. Infiltration and duct pressurization results	11
Table 2-3. Calibration heating load line coefficients, Q (Btuh) = $a \times T$ (°F) + b	15
Table 2-4. Estimated deadband, heater capacity, maximum cycling rate, and capacitance, by house, pre-HP	18
Table 2-5. Estimated deadband, heater capacity, maximum cycling rate, and capacitance, by house, HP testing, DHP	20
Table 2-6. Estimated deadband, heater capacity, maximum cycling rate, and capacitance, by house, HP testing, furnace	20
Table 2-7. Summary of heat pump manufacturer specifications	21
Table 2-8. Heat pump refrigerant line lengths	23
Table 2-9. Measurement instrumentation	30
Table 2-10. Inferred air flow equation coefficients for Systems A through F	34
Table 2-11. Quantity of temperature/humidity sensors by location and sensor type	34
Table 2-12. Building America internal gains estimate, 3 bedrooms, 1,206 ft ² conditioned area	40
Table 2-13. Sensible gain space heater schedule	41
Table 2-14. Latent load (humidifier) schedule	41
Table 2-15. CSA SPE-07 test room conditions for SCOPC test series	43
Table 2-16. CSA SPE-07 test room conditions for SCOPH rating test series	44
Table 2-17. Summary of testing periods	44
Table 2-18. CSA SPE-07 indoor air test conditions	45
Table 2-19. DOE Appendix M1 test conditions	45
Table 2-20. Heat pump field test conditions	45
Table 2-21. Cooling days, by system and temperature bin	46
Table 2-22. Heating days, by system and temperature bin	47
Table 2-23. Heat pump post-testing draw down refrigerant weights	49
Table 2-24. Differential pressure, inlet & discharge	49
Table 2-25. Types of heat pumps	53
Table 2-26. Values of A and C by system	55
Table 2-27. Table of variables	56



Acknowledgements

This report reflects the invaluable contributions of multiple individuals and organizations. This project is the result of a collaboration among a diverse range of heat pump market actors including regional energy efficiency organizations, energy efficiency program administrators, energy efficiency advocates and manufacturers. Northeast Energy Efficiency Partnerships (NEEP) enabled the partnership by serving as a facilitator, contributor, and fiscal agent.

Direct project funding contributions were provided by Air-Conditioning, Heating and Refrigeration Institute (AHRI), BC Hydro, CLASP, ComEd, New York State Energy Research and Development Authority (NYSERDA), Natural Resources Canada (NRCan), Northwest Energy Efficiency Alliance (NEEA), Pacific Gas & Electric (PG&E), Southern Cal Edison, and Xcel Energy.

With co-funding from this diverse range of organizations, NEEP facilitated the hiring of DNV as lead project researcher, Underwriters Laboratory (UL) to conduct lab testing, and Bruce Harley Energy to provide technical assistance.

NEEP would like to recognize the report's lead author from DNV, Jennifer McWilliams and DNV scope project manager Vivek Jaiswal. Lab testing was led by Mark Baines and Titus Mowry from UL Solutions. In-field monitoring and data analysis were led by David Yuill, Jim Butler, and Yuxuan Chen from University of Nebraska Lincoln (UNL), and Chris Williams from DNV. Bruce Harley Energy provided technical support and analysis.

Representatives from the funding organizations served as advisors throughout the project. NEEP would also like to recognize and thank members of the advisory committee for their review and input into the creation of this document.

Several leading heat pump manufacturers supported the project directly by assisting the lab testing, without which the project would not have been possible

Dave Lis, NEEP's Director of Technology Market Transformation, served as project manager. Formatting and edits were provided by Lisa Cascio, Director of Communications and External Relations, and Marianne Michalak of designMind.

About NEEP

NEEP was founded in 1996 as a non-profit whose mission is to serve the Northeast and Mid-Atlantic to accelerate regional collaboration to promote advanced energy efficiency and related solutions in homes, buildings, industry, and communities. Our vision is that the region's homes, buildings, and communities are transformed into efficient, affordable, low-carbon resilient places to live, work, and play.

Disclaimer: NEEP verified the data used for this report to the best of our ability. This paper reflects the opinion and judgments of the NEEP staff and does not necessarily reflect those of NEEP Board members, NEEP Sponsors, or project participants and funders.



Section 1: INTRODUCTION

This report details the first phase of a residential heat pump efficiency rating representativeness study conducted by DNV for Northeast Energy Efficiency Partnership. The study is part of efforts to modernize the metrics used to predict the in-field performance of heat pumps to protect consumer investments and utility incentive dollars and accelerate the electrification of heating systems across North America, an essential step toward decarbonizing everyday life and fighting climate change.

DNV performed field experiments and conducted preliminary data analysis to assess the representativeness of two heat pump testing and rating procedures:

- Air-conditioning, Heating and Refrigeration Institute (AHRI) 210/240-2023 (hereafter AHRI 210/240), used for regulation in Canada and the USA
- Canadian Standards Association (CSA) SPE-07:231 (hereafter SPE-07), which is being considered for regulatory adoption in Canada



DNV, working with the University of Nebraska-Lincoln (UNL), conducted experiments in Lincoln, NE, using three mobile homes and six heat pumps. The first phase (the “field” phase) of the study was conducted from March 2022 through February 2023.

The first phase report documents the field experiments, preliminary analysis of field-collected data, stakeholder access to data dashboards, and descriptions of second phase lab testing and analysis tasks. Lab testing and analysis comparing field-to-lab measurements will be performed in the second phase of the representativeness project managed by NEEP.

¹ The first edition of *Load-based and climate-specific testing and rating procedures for heat pumps and air conditioners*. It supersedes the document CSA EXP-07:19 of the same name



1.1 Study objectives

This study has two primary aims:

- Build a robust set of rigorous and well-controlled in-field measurement data to enable in-depth comparisons of the field data to the ratings produced by two major laboratory test procedures (SPE-07 and AHRI 210/240) for a set of ducted and ductless heat pumps².
- Determine the shortcomings or differences that diminish the relevance, or representativeness, of the lab test results compared with measured field performance.

1.2 Research questions

The primary research questions are:

- How well do the two laboratory test procedures available in North America represent field performance of heat pumps?:
 - CSA SPE-07:23: Load-based and climate-specific testing and rating procedures for heat pumps and air conditioners.³
 - Department of Energy (DOE) Code of Federal Regulations Title 10, Chapter II, Subchapter D, Part 430, Subpart B, Appendix M1 to Subpart B of Part 430⁴: Uniform Test Method for Measuring the Energy Consumption of Central Air Conditioners and Heat Pumps (January 2017), with references to the following standards:
 - ANSI/AHRI 1230-2010: Performance Rating of Variable Refrigerant Flow (VRF) Multi-Split Air-Conditioning and Heat Pump Equipment
 - ANSI/AHRI 210/240-2008: Performance Rating of Unitary Air-Conditioning & Air-Source Heat Pump Equipment
 - ANSI/ASHRAE 37-2009: Methods of Testing for Rating Electrically-Driven Unitary Air-Conditioning and Heat Pump Equipment
 - ANSI/ASHRAE 41.1-2013: Standard Method for Temperature Measurement
 - AMCA 210-2007: Laboratory Methods of Testing Fans for Certified Aerodynamic Performance Rating
 - ASHRAE 41.2-1987: Standard Methods for Laboratory Airflow Measurement
 - ASHRAE 41.6-2014: Standard Method for Humidity Measurement
 - ASHRAE 116-2010: Methods of Testing for Rating Seasonal Efficiency of Unitary Air Conditioners and Heat Pumps

² Note that the Department of Energy (DOE) “Appendix M1” is the governing document that the study will be testing to in the lab. Appendix M1 is harmonized generally with AHRI 210/240 as explained further below. Technically, field test conditions include (or are at least very close to) conditions set by Appendix M1, and there will be attention focused on adjusting or normalizing for different operating conditions, both indoors and outdoors.

³ Note that while the original targets for house UA and capacitance were based on the earlier standard CSA EXP-07:19, the lab test was always intended to use SPE-07:23. The load line and capacitance targets did not change between those versions, so SPE-07 is referenced throughout this report even though it was unpublished at the outset of the project.

⁴ Appendix M1 is harmonized generally with AHRI 210/240 but M1 is the governing document tested to in the lab

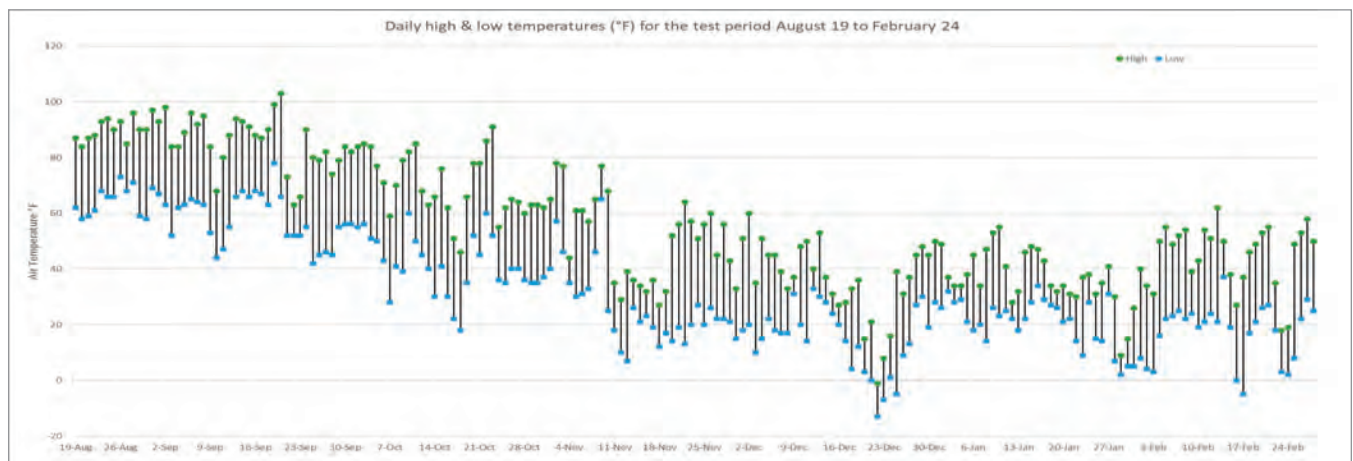


- ASHRAE 23.1-2010: Methods of Testing for Rating the Performance of Positive Displacement Refrigerant Compressors and Condensing Units That Operate at Subcritical Temperatures
- ASHRAE 41.9-2011: Standard Methods for Refrigerant Mass Flow Measurements Using Calorimeters
- Does the dynamic testing procedure used in CSA SPE-07:23 lead to ratings that better reflect in situ efficiency performance of heat pumps compared with the fixed speed testing methodology used in the DOE Appendix M1 and described by the AHRI 210/240 test standard? If yes, is the difference significant enough to justify broad adoption of load-based testing that results in climate-specific ratings?
- Could either (or both) test procedures be modified to better reflect performance expected in installed systems?
- Are there heat pump performance characteristics that should be (but are not currently) measured and factored into heat pump efficiency metrics that could easily improve the relevance of one or both test procedure results to performance in the field?
- Do the added heat pump performance characteristics that might enhance either or both test procedure results differ between the heating and cooling seasons?
- Do the laboratory rating procedures evaluate heat pump performance characteristics such as variable speed/multi-speed control strategies, and/or air handler fan operation?
- Are the identified performance characteristics equally applicable to both ducted and ductless heat pumps?
- Is low speed performance a significant indicator of variable-speed heat pump heating and/or cooling performance?

1.3 Study overview

DNV commissioned three identical, new mobile homes in Lincoln, Nebraska, for the duration of the mobile home calibration and both the cooling and heating measurement periods. The cooling measurement period was delayed and spanned from August to October 2022. The heating measurement period spanned from October 2022 to February 2023. Figure 1-1 visualizes the daily temperatures through the measurement period.

Figure 1-1. Daily temperature, high and low, in °F





Each mobile home had two air-source heat pumps installed: one ducted and one ductless. The mobile homes were also modified (to the extent possible) to mimic the thermal properties prescribed by CSA SPE-07, typical of building load profiles for single-family residences based on the rated heat pump size. All three mobile homes were similarly oriented, weatherized, and commissioned, with similar exterior shading and wind exposure conditions. Infiltration, conduction, and capacitance calibration tests were conducted to (1) measure existing condition of the mobile homes and to (2) guide thermal alterations to more closely match CSA SPE-07 properties. Building load profiles and capacitance were also estimated from data collected during the heat pump measurement period. These parameters are critical to reasonably compare the field data with results from the subsequent laboratory tests.



Section 2: MEASUREMENT AND VERIFICATION ACTIVITIES

2.1 Test site description

DNV rented three mobile homes in Lincoln, Nebraska. Lincoln was chosen because it meets the conditions⁵ dictated by the project design:

- Cooling tests to be performed at an elevation between 500 and 1,500 ft above sea level: Lincoln is at an elevation of 1,190 ft above sea level
- Cooling tests to be performed where it is reasonable to expect that temperatures will sometimes equal or exceed 95°F:
 - The 0.4 percent cooling design temperature in Lincoln is 96.6°F dry bulb and 74.9°F wet bulb
 - Typical Meteorological Year version 3 (TMY3) data for Lincoln indicates 40 annual hours at or above 95°F
- Heating tests to be performed where the heating design temperature is approximately 5°F: The 99% heating design temperature in Lincoln is 2°F
- Proximity to a major university that performs HVAC research

The three homes have the same floor plan and are of the same vintage (new at the time of rental). Each home's floor is approximately 16 ft x 76 ft in dimension, with an approximate area of 1,216 ft². The homes are close to one another and have similar orientation. They are sufficiently spaced and oriented to have similar solar load and wind exposure. Their locations are illustrated on the map shown in Figure 2-1. Homes located on lots 58, 162, and 272 were selected for this study.

Figure 2-1. Map of mobile home community in Lincoln, NE – selected homes circled in red

(image source: Havenpark Management)



⁵ Interactive map of ASHRAE design conditions is available at <http://ashrae-meteo.info/v2.0/>. Design temperatures are from the 2017 ASHRAE Fundamentals handbook, chapter 14. No cities in the United States met all the suggested design criteria (elevation 500-1,500 ft, 99% heat < 5°F, %1 cooling > 95°F).



2.2 Mobile home infiltration, conduction, and capacitance

The homes were tested and calibrated to approximate the target thermal characteristics of SPE-07 by iteratively performing the three tests described below and adjusting the home properties until the UA for all homes were within 5% of the home with the largest UA value. The starting point was not far from the SPE-07 target.

The blower door and duct leakage tests were performed first, then the conductance and capacitance tests. Fortunately, enclosure and duct air leakage rates across all homes were within reasonable ranges [3.5 – 4.4 ACH50] and within 25 percent of the home with the lowest leakage. Given the low leakage rates, the advisory team agreed that the homes did not require air or duct sealing.

The dynamic pulse test and the co-heating test were performed alternately; the thermal mass and the conductance were adjusted initially and during the measurement period to attempt to match the load lines and the time constant set in the SPE-07 standard. The calibration metrics calculated and reported are shown in Table 2-1.

Table 2-1. Study calibration metrics

#	Metric	Units
1	UA	Btu/hr/°F
2	Time constant	Hours
3	Infiltration rate	CFM50
4	Normalized infiltration rate	CFM50/ft ²
5	Supply duct leakage to outside	CFM25
6	Shallow mass capacitance	Btu/°F
7	Cycling rate	Hours ⁻¹

Calibration followed the steps below:

1. Blower door tests (pressurization and depressurization)
2. Duct pressurization tests (duct leakage to outside while house is pressurized equally)
3. Underbelly pressure with respect to outside
4. Manual-J measurements
5. “Baseline” co-heating (conduction) test
6. Adjustments to building shell to change UA
7. Re-test and finalize co-heating (conduction)
8. Dynamic Pulse (capacitance) test



2.2.1 Infiltration test

Blower door and duct leakage pressurization tests were conducted on March 2, 2022, and followed the test procedures documented in the Calibration M&V plan. Testing day was relatively warm for the season, with an average wind speed of 7 mph. ASTM E779-19 (“The Standard Test Method for Determining Air Leakage Rate by Fan Pressurization”) guidance was followed, and the tests were conducted during periods of relatively low and consistent wind speed.⁶ Differences between indoor and outdoor temperatures were negligible, and final leakage rates were not adjusted to compensate for air density differences.

House 2 and House 3 had nearly identical infiltration rates at 50 Pa. House 1 was the leakiest at 703 CFM50, which was 25 percent higher than the lowest infiltration rate of House 3 at 564 CFM50.

Duct leakage values for the three homes were all 5-6 percent of floor area, with House 2 having the lowest leakage rate at 57 CFM25.

Attempts to bring leakage rates to within 10 percent of other houses were not made because of time sensitivity to perform the conductance and capacitance tests. DNV, in collaboration with the technical advisory committee, agreed that the initial infiltration tests showed that the mobile homes were sufficiently tight and reasonably similar as to not require adjustments (i.e., air sealing) because other adjustments were anticipated that would impact the overall UA.

Table 2-2. Infiltration and duct pressurization results

Metrics	House 1	House 2	House 3
CFM50 (depress)	703	569	564
CFM50 (press)	906	809	844
CFM50/ft ² (depress)	0.58	0.47	0.46
Duct Leakage (CFM25)	77	57	79
Underbelly Pressure (Pa) (with respect to house)	2	3.1	1.7
ACH50 (depress)	4.4	3.5	3.5

⁶ ASTM E779-19 suggests wind speed should be less than 8.9 mph (4 m/s)



2.2.2 Co-heating (conduction) tests

The co-heating test is used to characterize the heat loss from the buildings. The basic principle of the co-heating test is that—due to conservation of energy when the thermal mass of the structure is maintained at a constant temperature—the energy flowing into the structure (electric heating energy, including internal gains from lights, appliances, or other equipment operating in the structure, plus solar gains through windows and solid surfaces) is equal to the heat energy lost to the outside.

At reference design conditions,⁷ the heat loss is equal to the design heating requirement, $DHR(T_j)$. The calibration tests were performed overnight initial co-heating tests and, iteratively, reduced the UA by installing galvanized sheet metal in the windows. Calibration adjustments were made based solely on the heating UA tests, and cooling load lines (and new heating load lines) were developed using heat pump capacity.

The goal was to get the buildings as close as possible to the CSA SPE-07 load lines for heating and cooling. Of greater importance, the goal of the calibration efforts was to align the steady-state heat loss rates across the three buildings within the 95% confidence interval. For reference, the CSA SPE-07 load lines are described by the following formulas:

Equation 2-1. Heating load line formula⁸

$$BL(T_j) = 1.15 \times \dot{Q}_c(95) \times \frac{T_{bal} - T_j}{T_{zl} - T_{ref}}$$

Where,

$BL(T_j)$ the building load at the test interval outdoor ambient dry-bulb temperature T_j

$\dot{Q}_c(95)$ the maximum total cooling capacity of the heat pump at an outdoor ambient dry-bulb temperature of 95°F as determined in the A or A2 test (as applicable), $BL(T_j)$ and $\dot{Q}_c(95)$ are in Btu/hr

T_{zl} the zero-load or design balance point temperature (60°F)

T_{ref} an outdoor load reference temperature = 5°F

T_{bal} the balance point temperature based on the current indoor room setpoint, which is updated according to:

$$T_{bal} = T_{zl} + (RAT(t) - T_{ID})$$

Where,

T_{ID} = the indoor design dry-bulb temperature specified as the test unit thermostat setting

RAT(t) = the most recent indoor dry-bulb temperature setpoint for the indoor room reconditioning system.

⁷ Heating design conditions are specified at 70°F indoor temperature and 5°F outdoor temperature, based on the 5°F outdoor reference temperature used in SPE-07 and AHRI210/240, which is also close to but does not correspond to the 99% design condition for the site location (2°F) per ASHRAE Fundamentals 2017

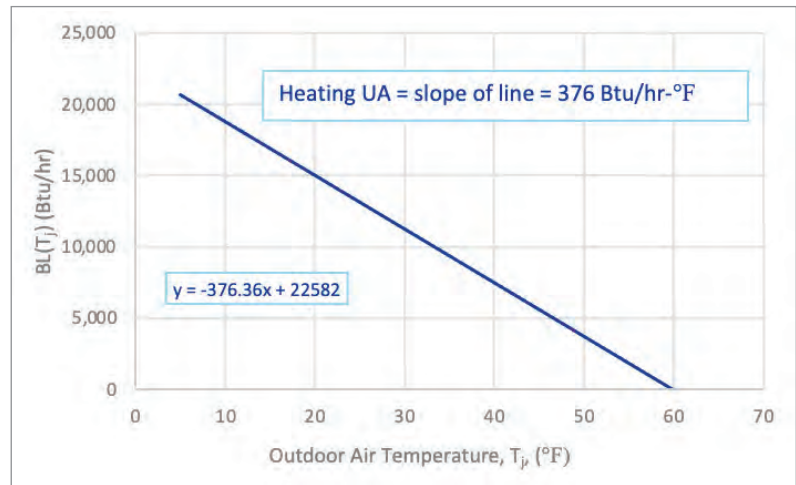
⁸ Equation B.9 of CSA SPE-07



Figure 2-2 shows the heating load as a function of outdoor air temperature, T_j based on Equation B.9 from SPE-07 shown above. The goal of the co-heating tests and calibration was to match the heating load line in Figure 2-2 as closely as possible and consider the range of capacities of the prospective equipment.

There was no attempt to calibrate to the cooling load line from CSA SPE-07 because cooling depends significantly on solar gains as well as outside temperature, and most critically because the cooling load cannot be met with simply measured devices, such as the electric heaters used for the heating UA test. We understood that the cooling loads would be whatever they would be in these houses and made no attempt to alter them beyond the alterations in the overall heating UA.

Figure 2-2. CSA SPE-07 heating load line as a function of outdoor air temperature



2.2.2.1 Calibration prior to heat pump installation

Calibration co-heating tests were conducted between March 3 and March 23, 2022. The houses did not yet have heat pumps installed, and minimal added thermal mass (testing equipment, shipping boxes) was present during the tests. The following test conditions were applied across all homes:

- Approximately 12 temperature sensors were deployed throughout each house to estimate an average indoor air temperature. Temperature sensors were arranged in vertical arrays to account for stratification and were placed in core and perimeter spaces (e.g., bedrooms, living/dining room, kitchen).
- Four 1,500W space heaters were deployed in each house with external thermostats set to maintain an 85°F set point with a tight 0.5°F dead band.
- Two ceiling fans, three box fans, and two oscillating pedestal fans were used to mix indoor air.
- After preliminary co-heating tests, the bottom sash of four windows in the core space (living/dining room area) of the homes were replaced with steel sheets to increase the UA. Three windows were south-facing and one window was north-facing.

House 2 had additional modifications that were not applied to the other houses:

- Approximately 4.5 ft² of supply ductwork was exposed under the house.
- Portions of the perimeter skirting (on all sides) were removed and replaced with chicken wire, to allow air to move under the house more freely.

These House 2 adjustments were initially made to measure their impacts relative to other conduction changes. Figure 2-3 through Figure 2-7 demonstrate the key changes made to the houses: (1) lower window sash replacement for all houses and (2) House 2 skirting removal and ductwork exposure.

The heating load lines measured during the calibration period are shown in Table 2-3 and Figure 2-7.

Figure 2-3. House 1 – north-facing window – lower sash replaced with sheet metal



Figure 2-4. House 1 – three south-facing windows – lower sashes replaced with sheet metal



Figure 2-5. Close up of lower window sash replaced with steel sheet metal



Figure 2-6. House 2 – Section of supply ductwork exposed to increase conductance





Figure 2-7. Heating load lines for all houses, calibration period

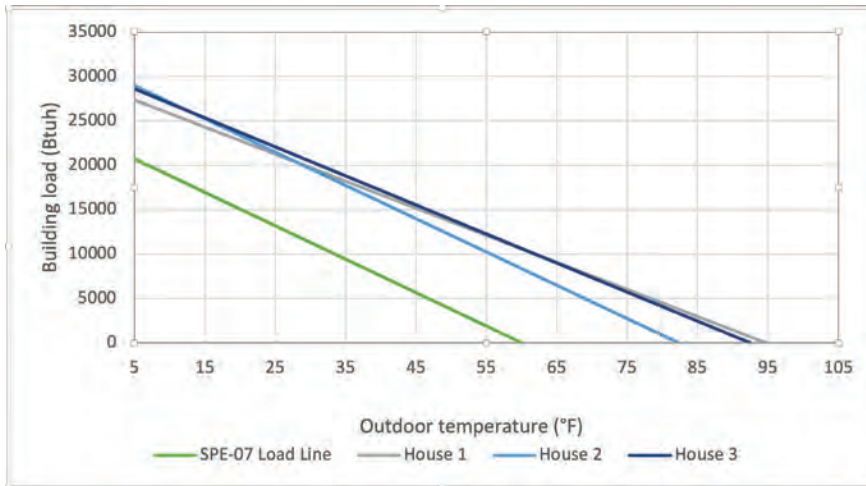


Table 2-3. Calibration heating load line coefficients, $Q \text{ (Btuh)} = a \times T \text{ (°F)} + b$

	a	b
CSA Load Line	-376	22582
H1	-305	28910
H2	-375	30867
H3	-327	30242

2.2.2.2 Heat pump test period

Load line analysis results are reported in Phase 2 report. It should be noted that the load lines being analyzed are the actual net loads seen by each heat pump, which include internal and solar gains and other transients over the test period, which is needed to best duplicate the field conditions for the load-based lab test. DNV is working with the technical advisory committee to provide load lines to use in Phase 2 lab testing.

2.2.3 Capacitance tests

The capacitance test is used to characterize the thermal capacitance of the houses. The thermal capacitance can be considered as having two components: shallow mass that readily participates in thermal energy exchange with the indoor air and deep mass that can store large quantities of energy but does not easily exchange thermal energy with the indoor air. In this study we are more interested in characterizing the shallow mass than the deep mass because the shallow mass is what dominates the building behavior during the off periods between heating or air conditioning cycles.

To characterize the shallow mass for initial house calibration, a dynamic pulse heat test was conducted during which the electric furnace was cycled to maintain an indoor setpoint temperature with a relatively wide swing. Section 2.2.3.1 discusses the test method and results that informed the team of the houses' initial thermal



capacitance and direction to adjust thermal capacitance for the HP testing period. Section 2.2.3.2 then discusses the thermal capacitance measured during the HP testing period. The capacitance tests utilize the following relationship between capacitance, heat gain, and thermostat properties⁹:

Equation 2-2. Capacitance equation

$$C_s = \frac{1}{4} \times \frac{\dot{Q}_{h,s,D}}{N_{max} \times \Delta T_{db}}$$

Where,

C_s The thermal capacitance [Btu/°F]

$\dot{Q}_{h,s,D}$ Heater capacity [Btu/h]

N_{max} Maximum cycling rate [1/h]

ΔT_{db} Thermostat deadband [°F]

The relationship between the cycling rate (N), N_{max} , and the run time fraction (X) is:

Equation 2-3. “Cycling rate” equation

$$N = 4 \cdot N_{max} \cdot X \cdot (1 - X)$$

The purpose of this test is to estimate the thermal capacitance of the building by measuring 1) the heat added to the space, 2) the variation in indoor temperature, and 3) the outdoor temperature as the heater cycles, providing a step function heating input. The data from the test was processed to provide the effective thermal capacitance and the time constant based on the maximum cycling rate at runtime fraction of 0.5.

2.2.3.1 Calibration prior to heat pump installation

The target shallow mass capacitance was 677 Btu/°F for the three mobile homes. More important was a focus on achieving capacitance across the houses that were within 10 percent of each other. During the calibration tests, the thermal mass was increased using six five-gallon buckets of water with lids. They were located near the electric furnace supply registers. The built-in electric furnace and its wall thermostat was set to heat the house to 85°F and ceiling, box, and pedestal fans were set to circulate air within the house.

To calculate the thermal capacitance the following building and HVAC characteristics were identified:

- The total heat provided by the electric furnace to the indoors
- The equipment maximum on/off cycling frequency
- The thermostat deadband

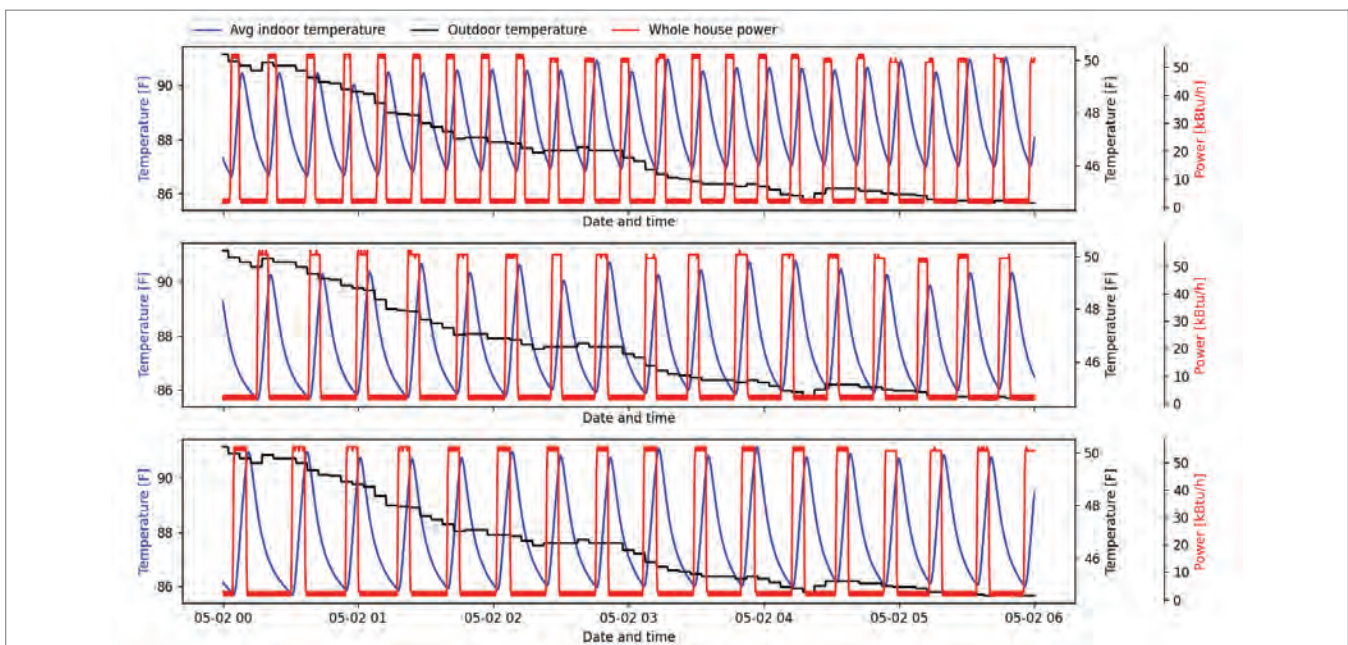
In the following paragraphs, we will describe how each parameter was identified.

⁹ ‘Measuring Thermostat and Air Conditioner Performance in Florida Homes’ by Henderson, H. et al, May 1991

The thermostat deadband:

It is important to highlight that the thermostat ΔT_{db} deadband involved in the calculation of the thermal capacitance is different from the thermostat deadband set to control the heater. Thermostat deadband is calculated as the average difference between the maximum and minimum of the measured indoor temperatures.¹⁰ Figure 2-8 shows an example of the average measured temperature for one night for the three houses. Due to measurements uncertainties and sensors’ location, the temperature extrema for each sensor may be reached at different times, which makes the deadband, calculated based on the averaged signal, slightly variable from cycle to cycle.¹¹ Also note that the left y-axis is indoor temperature, and the right y-axis is outdoor temperature.

Figure 2-8. Example of heater cycles and deadband for Houses 1, 2, and 3 (top to bottom)



In the thermal capacitance calculations, we used the calculated average deadband temperature over all the nighttime cycles for each home. Calculated values are given in Table 2-4.

¹⁰ Several RTD temperature sensors were deployed throughout the house. The temperatures were then averaged together to represent the average indoor air temperature
¹¹ A period during which the heater has been in successive on and off states.



Table 2-4. Estimated deadband, heater capacity, maximum cycling rate, and capacitance, by house, pre-HP

	House #1	House #2	House #3
ΔT_{db} [°F]	3.66	4.41	4.9
$\dot{Q}_{h,s,D}$ [Btu/h]	53,181	54,123	54,458
N_{max} 95% confidence interval	[6.43 – 7.19]	[5.13 – 5.85]	[4.69 – 5.16]
R ²	0.96	0.96	0.98
C_s 95% confidence interval	[505 – 565]	[524 – 597]	[537 – 591]

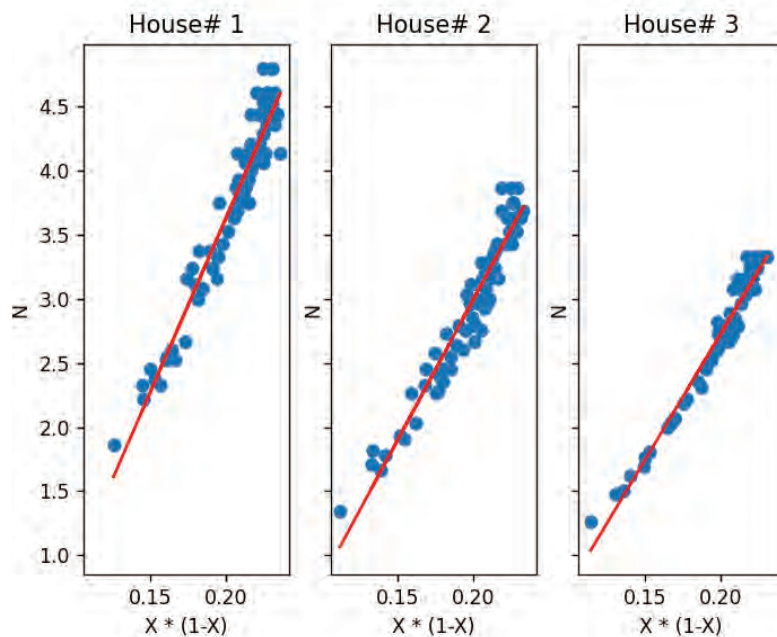
The indoor heating capacity:

The heat provided by the electric furnace $\dot{Q}_{h,s,D}$ to the indoors was calculated for each cycle as the maximum measured house total power minus the baseloads when the furnace was off and then averaged over all cycles for each house. Calculated values are given in Table 2-4.

The maximum cycling ratio:

Equation 2-3 shows the mathematical relationship between the runtime fraction, the cycling rate, and the maximum cycling ratio for each cycle. The runtime fraction, noted X , is defined as the ratio between the runtime duration and the cycle duration. The cycling rate, noted N , is defined as the number of cycles per hour and can be calculated as the inverse of the cycle duration in hours. The maximum cycling rate N_{max} , can be seen as the slope of the linear regression model, see Figure 2-9, divided by four. Coordinates of each data point in the figure were calculated based on a single heating cycle.

Figure 2-9. Scatter plot of N vs. $X(1-X)$ for each house





The regression analysis results and thermal capacitance with 95 percent confidence bands are given in Table 2-4.

The calibration target that the three houses have measured values of UA and C within 10 percent of the values assumed in the SPE-07 test ($UA = 376 \text{ Btu/h-}^\circ\text{F}$ and $C = 677 \text{ Btu/}^\circ\text{F}$). The houses' thermal capacitance ranged from –25 percent to –12 percent lower than the SPE-07 target.

Further adjustments to shallow thermal mass were not possible during the calibration period. Delays to the heat pump testing schedule were already impacting the cooling measurement days available in 2022. Based on the capacitance measured during the calibration period, the advisory committee estimated the additional thermal mass necessary to increase each houses' capacitance to the SPE-07 target. The adjustments were added on August 18, 2022, before the heat pump cooling measurement period began.

2.2.3.2 Heat pump testing period

The general guidance from the advisory group was to add shallow mass using drywall sheets separated with air gaps before the heat pump testing period. The water buckets used in the calibration testing were removed prior to heat pump testing.

The impact that the drywall additions had on thermal capacitance were measured during the heat pump testing period. Not only was drywall added to conditioned spaces, but the heat pumps, instrumentation, and left-over packing materials (cardboard boxes, Styrofoam, bubble wrap, etc.) were contained in the houses and acted as shallow thermal mass.

The advisory committee collectively agreed to use drywall as our method to add shallow mass. Exposed surface areas in a typical house were estimated to be between 5.5 to 6.5 ft² surface area (including ceiling and floor) per unit floor area.¹² The mobile homes were estimated to have approximately 5,700 ft² of interior surface area, including interior walls, ceiling, floor, and doors.¹³ By this measure, it was estimated that approximately 1,000 to 2,200 ft² additional surface area be added to the homes. This additional surface area was added by installing 16 sheets of 4' x 8' (1/2") drywall – a total of 1,024 ft² (includes both sides of the drywall). The sheets were cut into manageable sizes and distributed throughout the three bedrooms and the main living room area.¹⁴ Examples of these additions are shown in Figure 2-10 and Figure 2-11.

¹² Advisory committee members' experience decided on this range with reference to a 2021 study- Dhillon, Parveen; Welch, Drew; Butler, Brian; Horton, W. Travis; and Braun, James E., "Validation of a Load Based Testing Method for Characterizing Residential Air-Conditioner Performance" (2021). International Refrigeration and Air Conditioning Conference. Paper 2257; <https://docs.lib.purdue.edu/iracc/2257/>

¹³ The mobile home floor area is 1,216 ft²

¹⁴ Six full sheets in the living room, eight half sheets in BR1, and six half sheets each in BR2 and BR3

Figure 2-10. Drywall sheets installed in living room area to increase shallow thermal mass



Figure 2-11. Drywall sheets installed in “bedroom 1”



Final results of the capacitance analysis for the heat pump testing period are reported in the Phase 2 report. Preliminary results have shown that capacitance increased beyond the calibration period estimates, across all houses. Capacitance measured from field data are critical inputs for Phase 2 lab tests. Capacitance values used in the lab testing are reported in the Phase 2 report.

Table 2-5. Estimated deadband, heater capacity, maximum cycling rate, and capacitance, by house, HP testing, DHP

	House #1	House #2	House #3
ΔT_{db} [°F]			
$\dot{Q}_{h,s,D}$ [Btu/h]			
N_{max} 95% confidence interval			
R2			
C_s 95% confidence interval			

Table 2-6. Estimated deadband, heater capacity, maximum cycling rate, and capacitance, by house, HP testing, furnace

	House #1	House #2	House #3
ΔT_{db} [°F]			
$\dot{Q}_{h,s,D}$ [Btu/h]			
N_{max} 95% confidence interval			
R2			
C_s 95% confidence interval			



2.3 Heat pump installation and ductwork

Heat pump installation and commissioning occurred in phases:

1. Indoor unit and outdoor unit positioning and mounting
2. Electrical connections
3. Mass flow sensor integration with refrigerant line sets
4. Refrigerant line connections and commissioning (e.g., holding vacuum, checking for leaks)
5. Installation of measurement sensors
6. Start-up and follow-up tasks

Table 2-7 identifies the six heat pumps used in the study. Three ducted and three ductless heat pumps were selected by the technical advisory committee based on multiple factors, including availability, cold-climate rating and capacity, and manufacturer willingness to participate and donate for the study. System IDs were assigned to the heat pumps and are used frequently throughout the report. UNL also recorded line set lengths and the relative height difference between the indoor and outdoor units for all heat pumps.

Table 2-7. Summary of heat pump manufacturer specifications

System ID	House	Type	Cooling Capacity (nominal tons)	Heating Capacity (kBtu/h @5°F)	SEER	HSPF
A	1	Ducted	2	20	20	13
B	2	Ducted	2	10	16	
C	3	Ducted	1.5	22	18	10
D	1	Ductless	1.5	22	20	10
E	2	Ductless	1.5	17	22	13
F	3	Ductless	1.5	23	21	13

The heat pumps and duct work were installed by UNL and contracted HVAC technicians and commissioned by DNV and UNL staff. This section summarizes the out-of-box conditions of each heat pump, the procedures of installation, and issues each installation encountered. Instrumentation is discussed in Section 2.4. Note that the installations relied on out-of-box materials sent by the manufacturers and factory charge would be used unless otherwise directed by the committee.¹⁵ The out-of-box materials were sent by the manufacturers according to the indoor and outdoor unit model numbers and pairing configurations deliberated and finalized by the technical advisory committee.

Positioning of the ducted heat pump indoor units (IDU) and ductless IDUs were identical across all houses. Single-head, ductless heat pump IDUs were installed on an interior wall (both sides of the partition are adjacent to conditioned space) near the middle of the home with the vanes set to remain in an open position throughout

¹⁵A small amount of charge was added to compensate for the additional line set volume due to the mass flow sensor

the testing period. The ductless heat pump IDU was in the open central space of the mobile home, containing the living room, dining room, and kitchen areas.

Figure 2-12. Ducted HP ductwork ends in utility room facing native furnace return



The IDU for the ducted systems was installed on the indoor side of an exterior wall adjacent to the ductless head unit in the same central space. One trunk duct approximately 12 feet long was used to direct the discharge air to a utility closet area where the “native” air handler’s return grille was located.¹⁶ The native air handler and its existing ductwork were used to distribute the air of the ducted heat pump. The native air handler’s thermostat was set to “fan = on” which allowed the air handler fan to operate continuously at a low speed without using the electric furnace. Ducted system air handlers are mounted on Labor Saver returns, which have filter slots. The ductwork was constructed of insulated flex duct and was hung just below the ceiling level inside the conditioned space. Balancing dampers were not installed in the supply trunk line and external static pressure was not adjusted to 125 Pa as indicated in Table B.3 of CSA SPE-07.¹⁷

To equalize the room conditions throughout the house as much as possible, additional air mixing was accomplished using:¹⁸

- Two ceiling fans: one in the master bedroom (BR1) and one in the living room
- Two box fans: one located at the door of BR1 and one at the mouth of the hallway leading from the living room to the second and third bedrooms (BR2 and BR3)
- Three oscillating pedestal fans: one in BR1 and one each at the doors of BR2 and BR3

Manufacturer-supplied thermostat controls (for ducted and ductless heat pumps) were wall-mounted at a height of approximately five feet above the floor, on an interior wall in the kitchen.

Line set and indoor unit were pressure tested with dry nitrogen and vacuum tested (300-500 microns for an extended time) to ensure that there were no leaks and to remove any moisture/impurities.

Refrigerant lines were insulated. PVC condensate lines with a trap were connected to the indoor coil drain pan. These lines drain to a common condensate drain.

¹⁶ The native air handler is the electric furnace that came pre-installed in the mobile home

¹⁷ 125 Pa for central HPs at full load flow. Different system parameters (e.g., low and mid-static systems) have different minimum external static pressure value⁵

¹⁸ See Section 2.4 for a floorplan diagram

Table 2-8. Heat pump refrigerant line lengths

System ID	House	Liquid line length (feet)	Vapor line length (feet)	Height difference (inches between base of indoor to base of outdoor)
A	1	8	16.5	64
B	2	9.7	23.5	59
C	3	14.75	15.75	12
D	1	12.6	12.7	70
E	2	8	16.5	64
F	3	14.2	13.6	40

The heat pumps did not have supplemental electric heat. Backup heating was provided by the native electric furnace (15 kW) using a thermostat that was mounted on the interior wall below the ductless heat pump IDU.¹⁹

2.3.1 House 1

Both units in House 1 had installation issues that are discussed below. The outdoor unit of A and indoor unit of D were initially installed but were removed and replaced with correct models that were ultimately tested.

System A was initially delivered on April 11, 2022, and had the following conditions:

- Previously tested
- No refrigerant
- Outdoor unit hail guard bent (Figure 2-13)
- Air handler filter case broken (Figure 2-14)
- Outdoor unit fins bent in several locations (Figure 2-15)
- Outdoor unit leaking refrigerant

Figure 2-13. System A bent hail guard



Figure 2-14. Broken latch on filter case



Figure 2-15. System A bent and damaged fins



¹⁹ This was the original location of the native furnace thermostat. The original thermostats that came with the homes were analog; they were replaced with digital thermostats

The outdoor unit (ODU) of the ducted heat pump was damaged either before or during shipment. The unit was installed and pressurized to test whether the damage was superficial and did not affect the integrity of the refrigerant lines. However, the system proved to be compromised when, after the first few days of operation, the refrigerant leaked out and the system shut down. A replacement unit was provided by the manufacturer and delivered to the test site on August 22, 2022. It was installed, and all metering instrumentation was moved over to the new unit on August 24, 2022. Figure 2-16, Figure 2-17, and Figure 2-18 show System A ODU, IDU, and its ductwork.

Figure 2-16. System A outdoor unit



Figure 2-17. System A indoor unit with mass flow sensor



Figure 2-18. System A indoor unit, showing duct

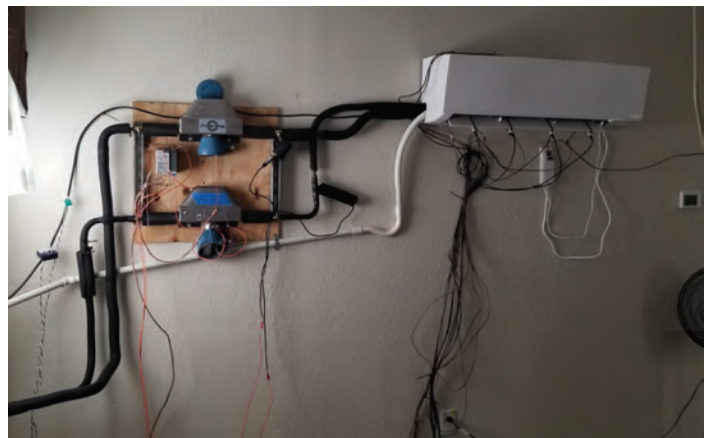


System D was delivered to the test site on June 23, 2022. The unit and measurement sensors were installed and operating under testing conditions for several weeks; however, the manufacturer’s wall thermostat could not interface with the indoor unit (the indoor unit was operating according to the remote controller and thermostat located on it). It was discovered in late September 2022 that the indoor unit that had been shipped was the incorrect model and was incompatible with the (correct) outdoor unit. Shortly after the discovery, the ductless heat pump indoor unit was replaced with the correct model. During this installation the outdoor unit was isolated with valves, and the piping and indoor unit were evacuated of charge. The charge that was removed was about five ounces, so an equivalent amount was added after the new indoor unit was installed and vacuumed. Testing data collection for the “correct” unit (System D) began on October 15, 2022.

Figure 2-19. System D outdoor unit



Figure 2-20. System D indoor unit with mass flow sensors



2.3.2 House 2

System B was delivered on site on June 23, 2022. Both IDU and ODU were new with no apparent damage. The IDU was delivered, installed and tested with a fixed orifice device, which inadvertently does not match the rated pairing combination for that unit configuration. When the IDU is paired with a two-stage ODU, a TXV accessory kit is required. For this reason, the manufacturer’s extended performance data are not relevant and will not be used in the analysis phase for this unit.

The outdoor unit came pre-charged and only 0.1 oz. was added to account for the volume in the mass flow sensor’s bypass path. A wall-mount (wired) thermostat was also provided to replace the remote wireless thermostat. The outdoor unit was positioned adjacent to a portion of the house where a panel section of underbelly skirting had been removed (to increase UA). We did not want the outdoor unit fan to draw in air from the underbelly, so the skirting panel (just the one panel) was re-installed.

Figure 2-21. House 2 – outdoor units and exposed underbelly



Figure 2-23. System B indoor unit



Figure 2-22. System B outdoor unit



Figure 2-24. System B indoor let set and mass flow sensor (not shown at bottom)



System E was delivered on site May 6, 2022. The unit was new and was inspected with no apparent damage. The outdoor unit came pre-charged; however, a faulty pressure gauge port leaked an unknown quantity of refrigerant after installation. We removed all refrigerant, evacuated, and weighed in the rated amount of refrigerant (4.08 lbs). A wired, wall-mount thermostat replaced the wireless, remote thermostat.

Figure 2-25. System E outdoor unit

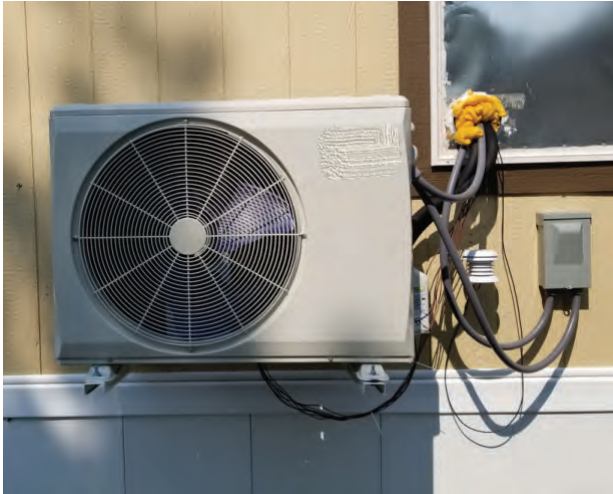
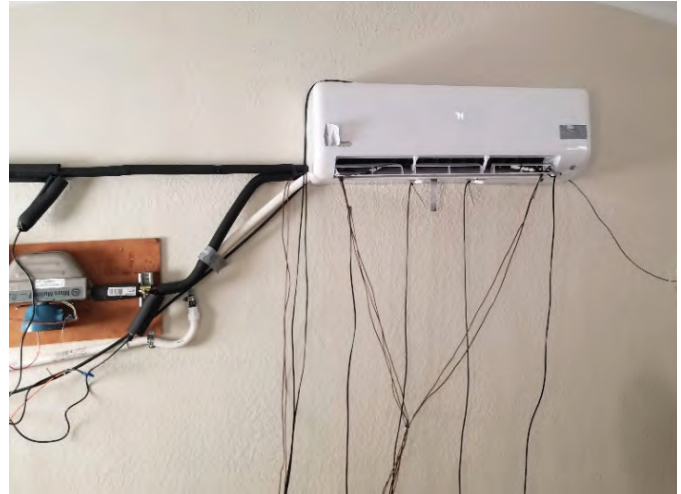


Figure 2-26. System E indoor unit with mass flow sensor



2.3.3 House 3

The ducted unit (System C) for house 3 was delivered new on-site May 11, 2022, with no apparent damage. The outdoor unit came pre-charged, and 0.1 oz. was added to accommodate the additional line length in the mass flow sensor bypass path. System C was the only ducted unit where the outdoor unit was mounted to the side of the house.

Figure 2-27. System C outdoor unit



Figure 2-28. System C indoor unit and duct



Figure 2-29. System C indoor unit line set and mass flow sensor



System F was delivered on site June 10, 2022. The indoor unit was damaged prior to being shipped to the site. Fins are bent, and a refrigerant tube in the heat exchanger is bent and slightly crimped. The filter is torn, and the plastic filter holder is broken. The manufacturer stated that they didn't expect the damage to affect the unit's performance. The outdoor unit came pre-charged and is mounted on the side of the house.

Figure 2-30. System F fin and tube damage



Figure 2-31. System F fin damage



Figure 2-32. System F indoor unit and mass flow sensor

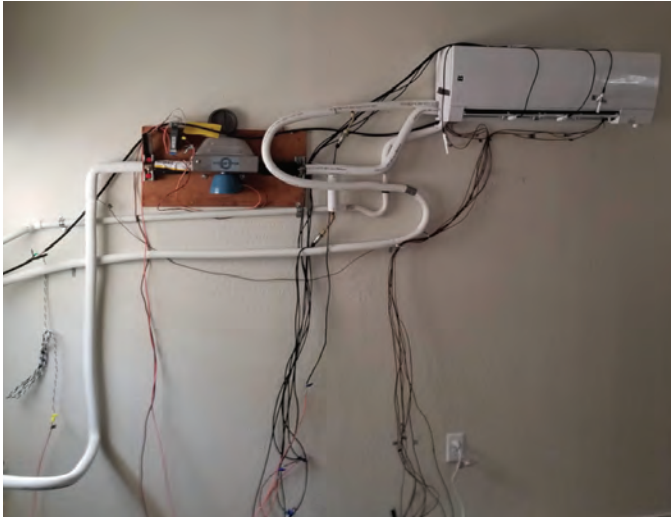


Figure 2-33. System F outdoor unit



Figure 2-34. System F ODU with shrouds removed, thermocouples and pressure gauges installed



2.4 Instrumentation installation

In collaboration with the technical advisory committee, DNV implemented the instrumentation strategy from the measurement and verification plan with minor changes in quantity and manufacturer. Instrumentation was nearly equivalent across all houses and heat pumps; differences lay in pressure sensor position. Positions were different because of inherent differences in pressure port locations. Table 2-9 shows the final installed quantity and position for each house and heat pump.



Table 2-9. Measurement instrumentation

Measured Parameter	Measured Points	Metering Equipment	Accuracy and Range
Electrical power (kW, kVA)	<ul style="list-style-type: none"> Total or Outdoor HP unit Indoor HP unit Native furnace House panel Water pipe strip heat 	eGauge Core power meters and CCS revenue grade CTs	<ul style="list-style-type: none"> Power meter: Class 0.5% CTs: Class 1.0%
Supply/outlet air temperature (T) and relative humidity (RH)	<ul style="list-style-type: none"> DHPs: (2) T/RH; (3) T-only DLHPs: (4) T/RH; (5) T-only 	<ul style="list-style-type: none"> Vaisala HMP113 temperature/RH probes (Modbus) Type-T thermocouples (Modbus) 	<ul style="list-style-type: none"> Vaisala: $\pm 0.1^{\circ}\text{C}$ at 20°C for temp; $\pm 1.5\%$ RH for the 0 to 90% RH range, and $\pm 2.5\%$ RH for the 90 to 100% RH between 0°C to 40°C; 15 second response Thermocouples: 1°C
Return/inlet air temperature and relative humidity	<ul style="list-style-type: none"> DHPs: (2) T/RH DLHPs: (2) T/RH 	Vaisala HMP113 temperature/RH probes (Modbus)	Vaisala: $\pm 0.1^{\circ}\text{C}$ at 20°C for temp; $\pm 1.5\%$ RH for the 0 to 90% RH range, and $\pm 2.5\%$ RH for the 90 to 100% RH between 0°C to 40°C ; 15 second response
Refrigerant-side pressure	<ul style="list-style-type: none"> DHPs: low side and high side DLHPs: low side and high side 	500 psig 4-20 mA pressure transducers	0.9% FS
Refrigerant-side temperature	<ul style="list-style-type: none"> 2-phase evaporator inlet Evaporator outlet Suction superheat True suction Discharge Discharge after reversing valve Liquid line inlet (3) Condenser tube bends 	Type-T thermocouples	1°C
Refrigerant Flow²⁰	Evaporator outlet / Condenser inlet	Emerson R025S or F025S	0.2% - 0.5%
Weather station	<ul style="list-style-type: none"> Temperature Humidity Wind speed Solar irradiance Barometric pressure 	Onset weather station	$0.2^{\circ}\text{C} / 2.5\%$ RH
Indoor ambient air temperature and relative humidity	<ul style="list-style-type: none"> (3) bedroom temperature and humidity thermostat temperature North wall cavity, drywall interior 	Onset wireless temperature/RH sensors (RXW-THC-900)	$0.2^{\circ}\text{C} / 2.5\%$ RH
Condensate Flow	Shared DHP/DLHP mL/min	Onset rain gauge (0.2mm)	4%
Internal gains	<ul style="list-style-type: none"> Scheduled and measured sensible gains Scheduled and benchmarked latent gains 		N/A
Indoor unit air flow, cfm	<ul style="list-style-type: none"> DHPs: differential pressure and calibrated flow plate DLHPs: Spot measured fan curve 		<ul style="list-style-type: none"> DHP dP sensor: 1% FS; 0-5VDC ($\pm 10\text{mV} \pm 0.3\%$ of reading) DHP flow plate: 7% at 365 cfm to 1,565 cfm DLHP: N/A

²⁰ DHP and DLHPs have (1) mass flow sensor each except for System D. System D has 2 mass flow sensors, one on each side of the indoor coil



DNV and UNL installed measurement instrumentation and began data collection for all three houses in August 2022. All sensors collected data in one-minute intervals. Sampling rates were one second or faster for all sensors.

A diagram of sensor position relative to mobile home floor plan is attached as a PDF in APPENDIX C.

DNV worked with the advisory group to agree on distribution of sensors and whether disparity between the ducted and ductless heat pump instrumentation was acceptable. There were minor differences in quantity and position of some temperature sensors. Ducted heat pumps had a total of two humidity sensors each on the indoor inlet and outlet, while the ductless heat pumps had two humidity sensors on the inlet and four humidity sensors on the outlet. The consensus that discharge air mixing is better in ducted than ductless systems led the team to decide to have more humidity sensors measuring the ductless discharge air. Condensate measurements will also be used to validate the latent capacity measurements over longer intervals for both ducted and ductless systems.

DNV used two methods for measuring unit cooling and heating capacity, for measurement assurance. The “air side” method measured the rate at which enthalpy is gained or lost by the air as it passes the indoor coil. The “refrigerant side” method measured the rate that enthalpy is gained or lost by the refrigerant during the cooling or heating phases. Note that the refrigerant side method can only measure total capacity, while the air side method is able to differentiate sensible and latent capacities. Because of its configuration, the ductless heat pump in House 1 (System D) had two Coriolis mass flow sensors installed—one on each side of the indoor coil—while the other heat pumps received only one, installed on the vapor line.

Missing data (the failure of transfer or loss of measurements from the sensor to the data acquisition device and DNV servers) was virtually non-existent. All data acquisition devices connected to a cable internet service provider via WiFi or wired network protocols. When missed connections occurred, sensor data was backlogged on the data logger’s local memory and pushed to DNV servers when connection was re-established.

A very limited subset of sensors experienced issues during the measurement period, i.e., bad data. Periods where the sensor accuracy or signal was compromised were recorded and documented. During the Phase 1 analysis, it does not appear that the sensor issues have compromised critical measurements for the study. Details on sensor issues are further explained in subsections 2.4.1 through 2.4.6. Phase 2 analysis will continue to investigate sensor anomalies and issues.

2.4.1 Power

Power measurements were measured using eGauge energy meters (Class 0.5 percent accuracy) and revenue grade split-core current transducers (CT, Class 1.0 percent). CTs were installed at the house’s electrical panel and wires feeding the indoor unit, and measured AC current with 333 mVrms output (see Figure 2-35 and Figure 2-36). The eGauge meters recorded AC real (W) and apparent power (VA) of the following circuits:

- Total panel (100A CT)
- Ducted heat pump outside unit²¹ (20A CT)
- Ducted heat pump inside unit (measured using one 1A CT and one 5A CT)
- Ductless heat pump total unit²² (20A CT)
- Ductless heat pump indoor unit (measured using one 1A CT and one 5A CT)
- Native furnace circuit (5A CT)
- Exterior water pipe heat tape (20A CT)

The native furnace circuit is a two-pole 60A circuit that feeds the electric furnace. The circuit powers the furnace’s control panel, fan, and two electric resistance coils (two stage heat). A CT rated to measure five amps was used to measure this circuit as a means for accurately measuring the native furnace fan power (rated at 3.6A). It does not accurately measure the electric furnace when the strip heat is energized. The electric resistance heat, when used as supplemental heat for the heat pumps, is measured indirectly using the total panel power.

Miscellaneous electrical loads (circulation fans, scheduled sensible space heaters, and measurement instrumentation) add heat to the house. They are measured indirectly by subtracting all other measured circuits from the total panel power. The exterior water pipe heat tape circuit is a single-pole 120V branch circuit that powers several wall receptacles in the house and a receptacle located in the underbelly powering a plug-in water pipe heat tape. This circuit was measured to allow subtraction of this outdoor electrical load from the total panel power to assess internal gains from electricity consumed inside the structure.

Figure 2-35. House electrical panel and CTs

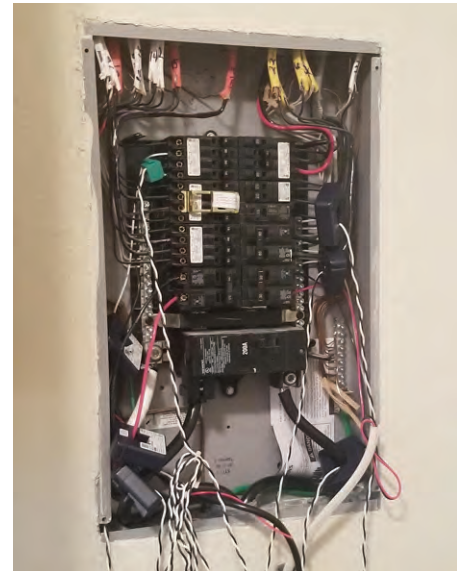


Figure 2-36. Two CTs (one rated 1A and one rated 5A) measuring indoor unit power



²¹ Systems A and B were powered with two 2-pole (240V) circuits. One circuit fed the outdoor unit and one circuit fed the indoor unit. System C was circuited with a single 2-pole circuit, feeding the outdoor unit. The system C indoor unit was fed from the outdoor unit.

²² All ductless systems were powered using a single 2-pole circuit that fed the outdoor unit. The indoor unit was powered from the outdoor unit

2.4.2 Airflow

Airflow was estimated using two techniques. Ducted heat pump airflow was estimated using calibrated Energy Conservatory TrueFlow[®] plates and 5-0 VDC differential pressure sensors. Using the differential pressure readings across the plates and the calibrated pressure-to-flow maps, volumetric flow rates are estimated from the differential pressure measurements. In System A and System B the filter slot is used to house the flow plates (see Figure 2-37). Filters were placed downstream of the flow plates. In ducted System C, the flow plate is installed in the indoor unit filter tray (and replaced the filter, see Figure 2-38)²³.

With flow plates and pressure sensors permanently installed, we were able to measure flow rates for ducted heat pumps throughout the testing period. There were some pressure sensor issues documented during the tests which compromised some periods of flow data. In addition to the measured flow rates, inferred flow rates were derived by mapping fan power to flow, during periods where we had high confidence in the accuracy of the pressure sensors (and thus flow rates), allowing correlation of measured flow rate to measured indoor unit power.²⁴

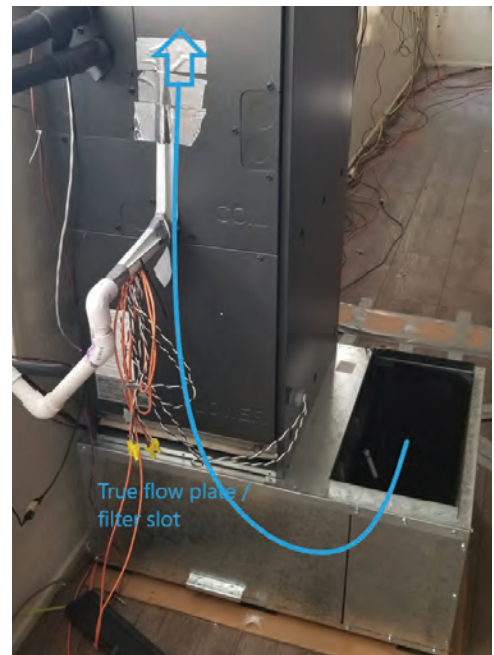
The ductless heat pumps had airflow measured using custom-made flow hoods, a calibrated Minneapolis DuctBlaster[®] fan, and a DG700-digital differential pressure manometer. With the flow hoods covering head unit outlet, the DuctBlaster[®] duct connected to the hood, and a static pressure probe inserted into a dead corner of the flow hood box, the ductless heat pumps were operated through all manually controlled fan speeds in cooling and heating modes. During each mode, the measured static pressure was counterbalanced with the DuctBlaster[®] fan so the static pressure measured zero, and the flow rate (through the DuctBlaster[®] fan) and IDU power were measured.

With these two methods, the ducted heat pumps have two reported air flows—measured and inferred—and the ductless heat pumps have one reported air flow—inferred. The inferred cubic equation and coefficients relating indoor unit power to air flow are shown in Equation 2-4 and Table 2-10. Derivation of the cubic equations listed below are provided in APPENDIX F.

Figure 2-37. Ducted HP flow plate in filter slot (system A and B)



Figure 2-38. System C flow plate position (filter cover removed to show plate)



²³ This means that System C was run without a filter

²⁴ Note that indoor unit power was measured and includes parasitic loads like control board power. The indoor unit can be drawing power when fan is off



Equation 2-4. Air flow cubic equation

$$q_{fan} = \left(\frac{Q_f - C}{A} \right)^{\frac{1}{3}}$$

Where,

q_{fan} = air flow in cfm

Q_f = measure indoor unit power in Watts

Table 2-10. Inferred air flow equation coefficients for Systems A through F

System	Type	Value of A	Value of C
HVAC A	Ducted	6.86E-07	22.4
HVAC B	Ducted	5.44E-07	9.65
HVAC C	Ducted	7.10E-07	4.16
HVAC D	Ductless	1.81E-07	8.52
HVAC E	Ductless	1.43E-07	6.46
HVAC F	Ductless	5.20E-07	4.81

2.4.3 Air temperature and humidity

Temperature and humidity (T/RH) instrumentation utilized several varieties of sensors. Sensors with higher accuracy and faster response times were used to measure indoor coil outlet/discharge conditions. Other sensors were utilized to measure temperature and humidity of stable air conditions (e.g., outdoor air, ambient space temperature). Table 2-11 shows the breakdown of sensors distributed throughout the houses.

Table 2-11. Quantity of temperature/humidity sensors by location and sensor type

Location	Vaisala HMP113 T/ RH; 0.1°C/1.5%RH; RS-485 Modbus RTU	Type-T thermocouple; 1.0 °C; RS-485	Onset T/RH sensors; 0.2 °C; 2.5% RH; digital	Onset T sensors; 0.2 °C; digital
Ducted HP indoor coil outlet	2	3		
Ducted HP indoor coil inlet	2			
Ducted HP outdoor coil inlet				1
Ductless HP indoor coil outlet	4	5		
Ductless HP indoor coil inlet	2			
Ductless HP outdoor coil inlet				1
Thermostat		1		
Bedroom 1			1	
Bedroom 2			1	
Bedroom 3			1	
South-facing exterior wall ²⁵				3
North-facing exterior wall				3
Interior wall				3
Weather station			1	

²⁵ An RTD temperature probe was placed on the interior wall surface, the wall cavity, and the cavity side interior wall surface. This was performed for a north-facing exterior wall, south-facing exterior wall, and interior wall.

An example of ductless HP indoor coil outlet sensor positioning can be seen in Figure 2-39.

Figure 2-39. System D temperature and RH sensor arrays

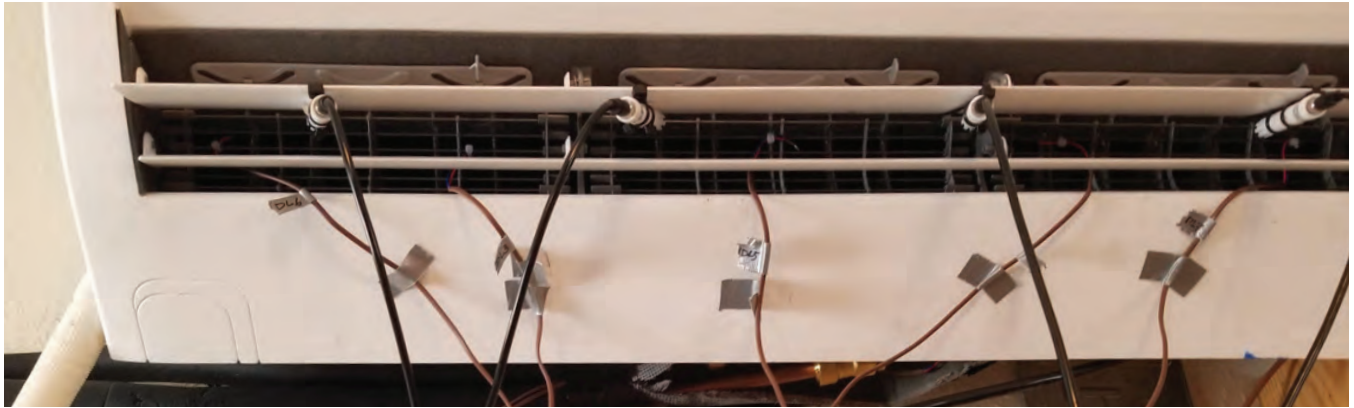


Figure 2-40. System D return/inlet temperature/ RH sensors



Figure 2-41. System C supply air plenum thermocouple array



Figure 2-42. Ductless HP supply/outlet air temperature/RH sensors



Figure 2-43. Ducted HP inlet air temperature sensor location



Figure 2-44. “Thermostat” thermocouple



Figure 2-45. “BR2” wireless temperature and humidity sensor



No T/RH sensors appeared to fail over the testing period, but there were instances where sensors became dislodged and fell outside of the measured air stream. Some of the instances were corrected relatively quickly during field visits to the houses. However, there were also some instances where it was not discovered until the decommissioning and removal of the sensors.

In addition to identified instances of sensor “displacement,” there were also subjective instances of sensor “misplacement” or sensors that appeared to not reasonably capture the air condition that it was intended to

measure. This occurrence appears to have only occurred with certain sensors in the coil outlet air streams, where the measured T/RH of the sensor was highly influenced by its position near the air stream, likely due to turbulence and non-laminar air flow patterns at the coil outlets, especially in the ductless units. Take for example the Vaisala sensors shown in Figure 2-46 and Figure 2-47 and labeled one to four. When the unit is off, all the sensors converge to the same temperature reading; however, when the unit is on, the sensors can vary in temperature reading by up to 20°C. The sensor readings are, unless flagged as anomalous, averaged together to represent the conditions of the coil’s outlet air, like temperature and enthalpy. Thus, the selection of which sensors best represent the conditions of the air stream are critical to estimating the unit’s air side capacity. We are continuing to document and analyze these findings and their impacts on calculated air-side capacity as well as validating them with refrigerant-side capacity measurements.

Figure 2-46. System F outlet T/RH sensors 1 through 4

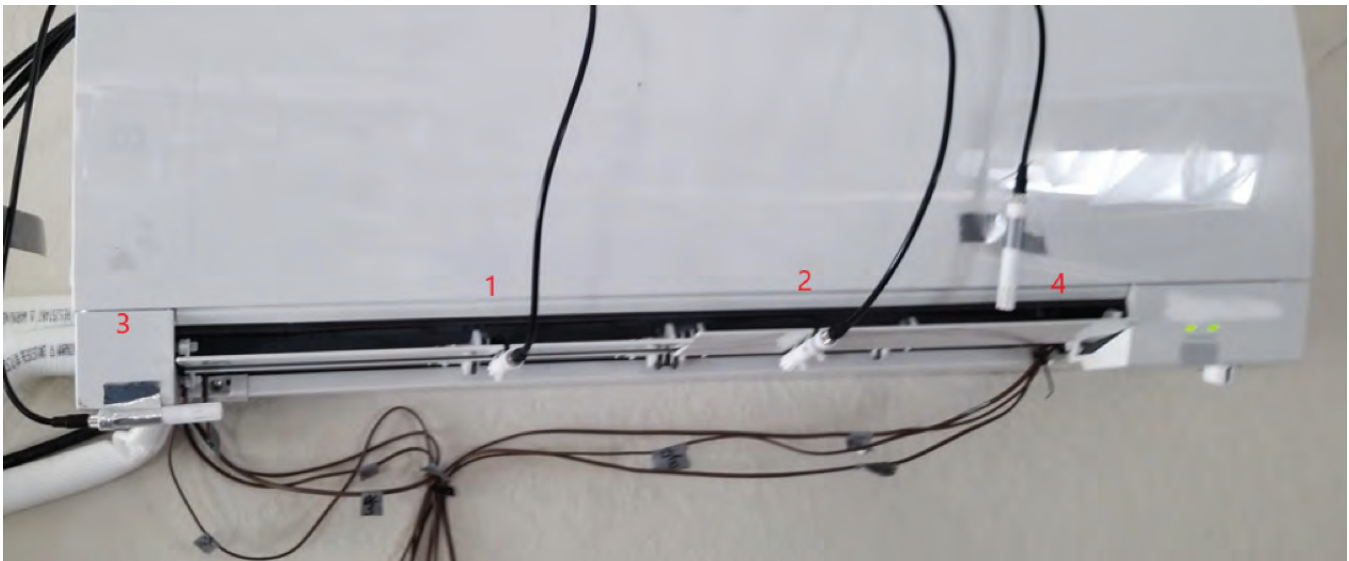


Figure 2-47. System F outlet T/RH sensors 1 through 4 readings



2.4.4 Refrigerant measurements

Refrigerant-side measurements were collected to estimate refrigerant state and refrigerant-side capacity. Two gauge pressure sensors rated for 500 psig are connected to each system. These are connected either with a short length of hose or a short brass fitting. We attempted to install the gauge pressure sensors in the same high and low side positions across systems. However, due to limiting factors like existing port locations, some systems had different sensor positions.

Mass flow sensors were positioned on the vapor line (compressor discharge in heating, suction in cooling). The exception is System D, which had mass flow sensors in both lines. The following locations along the refrigerant line were measured using Type-T thermocouples attached tightly and insulated:

- Indoor coil, inlet
- Indoor coil, outlet
- Superheated suction during cooling,
- Discharge after reversing valve (outdoor coil inlet during cooling, outlet during heating)
- Discharge
- Suction
- Liquid line (outdoor coil outlet during cooling, inlet during heating)
- Outdoor coil tube bends (three locations)
- Vapor line (discharge during heating, superheated suction during cooling)

The diagrams in APPENDIX D illustrate the location of sensors relative to heat pump components and line sets.

Preliminary refrigerant-side analysis by UNL has offered optimism regarding the accuracy and utility of the refrigerant mass flow measurements. Refrigerant-side measurements were taken to validate air-side capacity measurements and to assist with indirectly signaling for changing operating modes (e.g., defrost).

Figure 2-48 to Figure 2-52 show examples of refrigerant instrumentation installations.

Figure 2-48. House 1 ductless HP refrigerant mass flow sensors

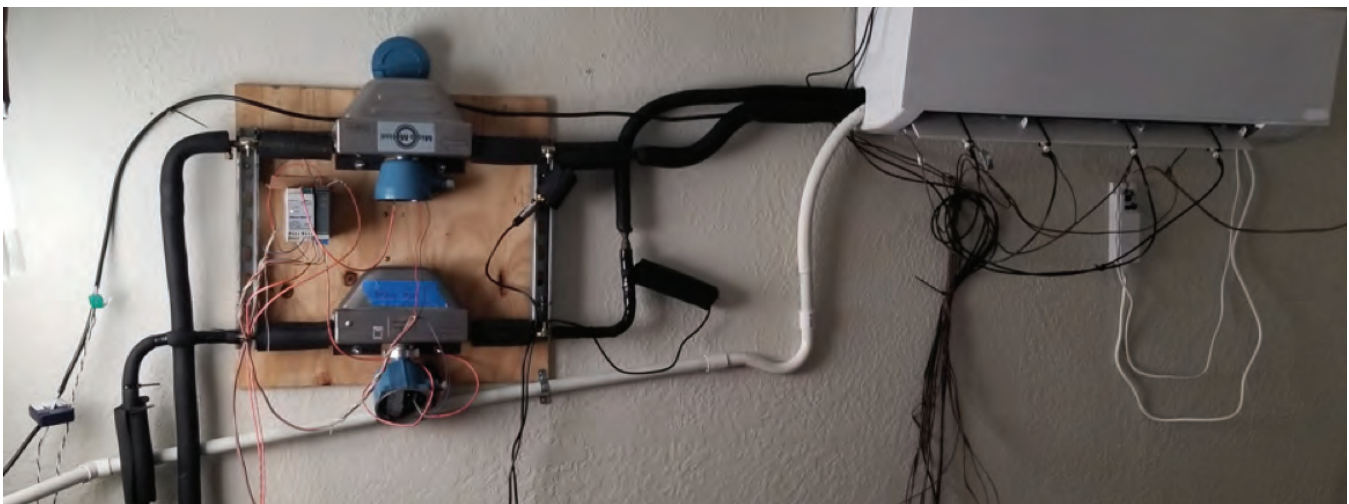


Figure 2-49. House 1 ducted HP refrigerant mass flow sensor

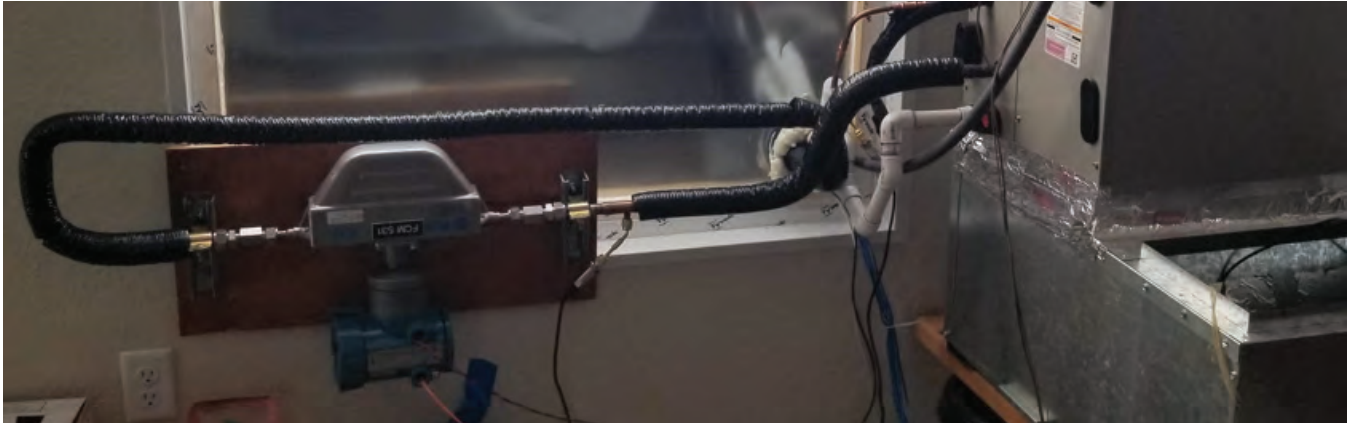


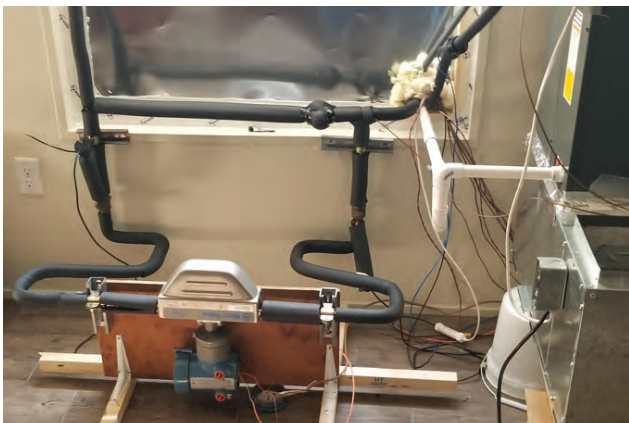
Figure 2-50. Ductless HP, pressure gauge T-tap



Figure 2-51. Ductless HP thermocouple, true suction



Figure 2-52. House 2 ducted HP refrigerant mass flow sensor and gauge pressure sensors





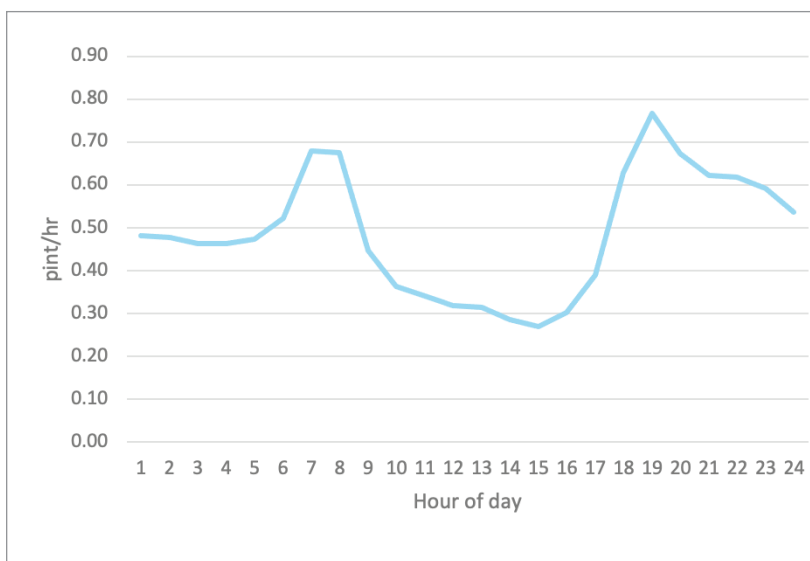
2.4.5 Internal gains

Scheduled internal gains were added to the houses using continuous, native sensible heat (from fans), electric space heaters, and humidifiers. Internal gains from the 2014 Building America House Simulation Protocols²⁶ were used to benchmark the internal gains schedules for the mobile homes. Internal gains from typical modeled household appliances, activities, and occupancy were aggregated to determine an average hourly sensible gain and a daily latent load shape.

Table 2-12. Building America internal gains estimate, 3 bedrooms, 1,206 ft² conditioned area²⁷

Internal Gain Type	Sensible Btuh	Sensible Watts	Latent pints/day
Showers	577	169	1.4
Sinks	241	71	0.3
Laundry	93	27	0.5
Dishwasher	41	12	0.3
Cooking	78	23	1.4
Misc. Electric	922	270	0.4
Occupants	402	118	7.4
Lights	385	113	1.4
Total	2,738	803	11.7

Figure 2-53. Daily latent load shape



²⁶ https://www.energy.gov/sites/default/files/2014/03/f13/house_simulation_protocols_2014.pdf

²⁷ https://www.energy.gov/sites/default/files/2014/01/f6/3_2b_ba_innov_housesimulationprotocols_011713.pdf



Table 2-13. Sensible gain space heater schedule

Sensible gain "on" schedule
1:00 AM
4:00 AM
7:00 AM
9:00 AM
11:00 AM
1:00 PM
3:00 PM
5:00 PM
7:00 PM
10:00 PM

Constant sensible gains in each house came from circulation fans and data collection equipment, totaling approximately 500W. The remaining ~300W (of constant sensible gain) was introduced using a scheduled 750W electric space heater. The space heater was scheduled using a smart plug to run 10 hours per day, spaced in one-hour intervals as shown in Table 2-13. For example, the heater turns on at 1:00 am and runs for one hour, turns off at 2:00 am, then turns on again at 4:00 am, runs for one hour, and turns off at 5:00 am. The majority of sensible gains were not controllable (due to the need for constant air circulation via the fans) and thus the research team spread the space heater schedule evenly over a 24-hour period and did not attempt to match the sensible load shape. The scheduled sensible gains were enabled on September 6, 2022 and ended on February 28, 2023.

Latent gains were modeled using a humidifier scheduled with a smart plug. The humidifier was positioned in the kitchen sink, and a float valve would fill the basin to keep the wet media consistently saturated. The humidifier’s rate of vaporizing water was benchmarked by weighing in the water container, running the humidifier for a set period, then weighing the container again.²⁸ The vaporization rate (1.63 lb. water/hr) was mapped to the daily latent load shape shown in Figure 2-53 to determine the smart plug schedule that would most closely align to the shape. The following schedule was used for the humidifier.

Table 2-14. Latent load (humidifier) schedule

Hourly total pint/hr	Minutes at 1.63 lb/hr	Schedule (24 hour)	
0.48	18	00:42	on
0.48	18	01:18	off
0.46	17	02:43	on
0.46	17	03:17	off
0.47	17	04:43	on
0.52	19	05:19	off
0.68	25	06:35	on
0.68	25	07:25	off
0.45	16	08:44	on
0.36	13	09:13	off
0.34	13	10:47	on
0.32	12	11:12	off
0.32	12	12:48	on

²⁸ The float valve was disabled during this period so the difference in water mass could be measured over an elapsed period



0.29	11	13:11	off
0.27	10	14:50	on
0.3	11	15:11	off
0.39	14	16:46	on
0.63	23	17:23	off
0.77	28	18:32	on
0.67	25	19:25	off
0.62	23	20:37	on
0.62	23	21:23	off
0.59	22	22:38	on
0.54	20	23:20	off
11.71	432	Totals	

The humidifier schedule operated from September 30 to October 25, 2022. The humidifier was turned off when the heating measurement period began.

2.4.6 Weather station

A weather station was installed on the front porch of House 1. While the measurements that the weather station provided are not expected to provide critical information, it did provide measurements that can help specifically characterize and bin particular operating periods, using:

- Wind direction and wind speed
- Solar irradiance (W/m^2)
- Barometric pressure

The weather station also measures outdoor dry bulb temperature and relative humidity.

Figure 2-54. Weather station located at House 1





2.5 Conduct tests

Mobile home testing started as soon as the HP systems and instrumentation were commissioned. The testing schedule was delayed due to multiple factors including heat pump commissioning issues (damaged units, leakage), shipment delays, and instrumentation delays (leaky connectors, mass flow assembly fabrication). Cooling tests were originally scheduled to start on June 1, 2022, but tests did not officially begin until August 19, 2022.

Further, there were delays in implementing the internal sensible and latent load schedules. Internal sensible loads (scheduled space heaters) were introduced in all homes on September 6, 2022, and internal latent loads (scheduled humidifiers) were introduced on September 30, 2022.

The indoor and outdoor conditions for the laboratory cooling and heating tests according to CSA SPE-07 are shown in Table 2-15 and Table 2-16 respectively.

Table 2-15. CSA SPE-07 test room conditions for SCOP_c test series

Test	Humid Test Conditions ⁱⁱ			Dry Test Conditions		
	Outdoor dry-bulb temperature, °F	Indoor dry-bulb temperature, ⁱⁱⁱ °F	Indoor humidity ratio ^{iv}	Outdoor dry-bulb temperature, °F	Indoor dry-bulb temperature, ⁱⁱⁱ °F	Indoor humidity ratio ^{iv}
CA ⁱ	N/A	74	0.010	113	79	0.0087
CB	104			104		
CC	95			95		
CD	86			86		
CE	77			77		

- i.) Temperature “CA” conditions are required only for a “Hot/Dry” climate rating.
- ii.) Outdoor humidity conditions during cooling mode tests where the system rejects condensate to the outdoor coil shall be selected to maintain an outdoor relative humidity of 40%. The values for humidity ratio are: 0.025 at 113 °F DB; 0.019 at 104 °F DB; 0.015 at 95 °F DB; 0.011 at 86 °F DB; and 0.0082 at 77 °F DB. For single-package systems where all or part of the indoor section is located in the outdoor test room, the average humidity ratio of the air entering the outdoor coil during wet coil tests must be within 0.0011 of the average humidity ratio of the air entering the indoor coil, over the convergence or measurement period used to calculate capacity and power input.
- iii.) Indoor room conditions at start of testing, target for equipment to meet during dynamic test intervals, and indoor room test temperature for full-load test intervals.
- iv.) Indoor room conditions at start of testing, and indoor room test condition for full-load test conditions.



Table 2-16. CSA SPE-07 test room conditions for SCOP_H rating test series

Test	Continental outdoor conditions		Marine outdoor conditions		Indoor conditions	
	Dry-bulb temperature, °F	Humidity ratio	Dry-bulb temperature, °F	Humidity ratio	Dry-bulb temperature, ⁱⁱⁱ °F	Humidity ratio ^{iv}
HB ⁱ	5	0.00080	N/A	N/A	70	0.0092 (max)
HC	17	0.0013	N/A	N/A		
HD	34	0.0031	34	0.0035		
HE	47	0.0042	N/A	N/A		
HF	54	0.0045	N/A	N/A		
HL ⁱ	LCT	ii	N/A	N/A		

- i.) Condition HL (LCT) is an optional test at the lowest catalogued temperature
- ii.) The humidity ratio for test HL, if conducted, shall be considered to be a maximum, and shall be calculated as $W = 0.000000543 * T_{DB}^2 + 0.0000357 * T_{DB} + 0.000554$, for the range of $LCT -24 \text{ °F} \leq TDB \leq 5 \text{ °F}$. For TDB below -24 °F , $W = 0.0000001$.
- iii.) Indoor conditions at start of testing, target for equipment to meet during virtual-load test intervals, and indoor room test condition for full-load test intervals.

Because of set-up and commissioning delays, the cooling test period was shortened. However, it was possible to extend the end of the cooling test period past the middle of October because of many hotter-than-normal days. While this also delayed the start of heating mode tests, we are confident that the test period included ample variation across a range of outdoor conditions to provide confidence in the applicability of the results for both cooling and heating tests. A summary of the testing period dates, and number of testing days are shown in Table 2-17. Detailed descriptions are further given in Sections 2.5.1 and 2.5.2.

Table 2-17. Summary of testing periods

Heating or Cooling	Start	End	# of days
Cooling	August 19, 2022	October 24, 2022	67
Heating	October 25, 2022	February 28, 2023	127

The research objective was never to characterize the heat pump performance for a particular year in a particular location; rather, it was to:

1. Develop performance profiles of the heat pump units over a wide temperature ranges and realistic loads and then apply the performance profiles to normalized weather bins;
2. Compare the heat pump systems' normalized seasonal performance profiles to those derived in laboratory testing based on the CSA SPE-07 and DOE-Appendix M1 lab performance test and rating protocols.

A summary of the indoor test conditions for CSA SPE-07 and Appendix M1 can be found in Table 2-18 and Table 2-19. The field test conditions (i.e., the thermostat set point) are shown in Table 2-20.



Table 2-18. CSA SPE-07 indoor air test conditions

Heating or Cooling	Dry or Humid Test	Indoor Dry-Bulb Temperature, °F	Indoor humidity ratio
Cooling	Humid	74	0.010
Heating	N/A	70	0.0092 (max)

Table 2-19. DOE Appendix M1 test conditions

Heating or Cooling	Air Entering Indoor unit dry-bulb temperature, °F	Air entering indoor unit wet-bulb temperature, °F
Cooling	80	67
Heating	70	(60 maximum)

Table 2-20. Heat pump field test conditions

Heating or Cooling	Heat pump thermostat set point °F	Backup electric furnace heating set point °F
Cooling	74	62-64
Heating	70	62-64

It is important to note that the field test conditions were set to match SPE-07 using the heat pump thermostats, but the actual room conditions the systems were controlling to were never calibrated to these temperatures so there was some variation which will be accounted for in the analysis phase. The backup furnace setting was to prevent the house temperature from dropping so much in cold weather that the heat pump performance for those hours would be seriously affected.

Internal loads were simulated as described in Section 2.4.5. The indoor humidity ratio was not controlled to the specifications outlined in Table 2-18 or Table 2-19, but was monitored, and controlled to the specifications developed for simulating internal loads. In the SPE-07 tests, indoor humidity ratio is not a controlled indoor room condition past the initial set-up of the psych chamber. After set up, the load-based test uses a virtual latent load model following an assumed sensible heat ratio of the total load, to introduce moisture as if it were a real house and lets the unit under testing control (or not) as it will while it responds to the thermostat. Humidity ratio is not maintained by the room conditioning equipment in a steady state as it is in M1, and the test results include reporting of humidity maintained during the test conditions.

2.5.1 Cooling

Cooling tests started across all houses on August 19, 2022. The entire suite of sensors was not fully installed or commissioned on that day but there were enough sensors to characterize heat pump power and capacity.

Table 2-21 shows the total number of cooling days collected for each system, binned into temperature ranges. Note that the numbers represented here only include days where in the data collection logs the day is marked as



“Good”. The data collection log qualitatively assigns days “Good,” “Caution,” or “Skip” to act as binary filters for including the data in analysis. Further investigation may change assignment of individual days and allow them to be included or excluded from the analysis.

Table 2-21. Cooling days, by system and temperature bin

Temperature bin, °F	System A	System B	System C	System D ²⁹	System E	System F
Above 94°F	3	4	3	N/A	5	5
86°F to 94°F	13	12	11	N/A	11	11
77°F to 85°F	11	9	7	N/A	10	10

During the cooling measurement period, the heat pumps held a constant set point temperature and were switched manually on and off to change between the ducted and ductless units periodically in each house. We elected to manually switch between heat pumps to carefully control how many days each heat pump operated during the shortened cooling period. We used weather forecasts to guide when we switch between heat pumps, to more evenly distribute days of various temperatures amongst the heat pumps. Heat pumps were generally switched over in the mornings (around 9:00 am³⁰).

Critical events during the cooling tests are noted below:

- Scheduled sensible space heaters were installed on September 6.
- Scheduled latent loads (humidifiers) were installed on September 30.
- From October 2 through October 13 the native furnace fans were inadvertently turned off. The native furnace fans were used to help distribute the ducted heat pump air, so when the furnace fan was off, it significantly impacted the load that the ducted heat pump responded to. The ductless heat pumps were less impacted because for them, the air supply was distributed throughout the main living space using the plug-in circulation fans.
- During the shoulder of the cooling season (October 14 to October 24), the native electric furnace heater turned on during some nights. The diurnal swing in daily temperature was considerable during the shoulder period, with daily temperatures as high at 91 °F and as low as 19 °F. The heat pumps were in cooling mode and thus did not switch to heating, but the maintenance of a warmer indoor condition at night ensured that there would still be useful cooling load during the day, and likely was more realistic regarding typical operation of occupied houses.

All documented events are detailed in the data collection summary in APPENDIX A.

²⁹ System D had a mismatched, incorrect indoor unit until October 15, 2022, and had a total 10 days of cooling measurement

³⁰ The cooling “day” for each date in the data collection log is from 9 AM to 9 AM the following day



2.5.2 Heating

The heating measurement period began on October 25, 2022. The table below shows the total number of heating days collected for each system, binned into temperature ranges. Note that the numbers represented here only include days where in the data collection logs the day is marked as “Good”.

Table 2-22. Heating days, by system and temperature bin

Temperature bin, °F	System A	System B	System C	System D	System E	System F
47°F to 54°F	8	8	6	16	16	10
34°F to 47°F	20	18	11	9	8	4
17°F to 34°F	50	46	26	39	38	22
5°F to 17°F	10	7	4	21	19	10
-10°F to 5°F	11	8	5	5	3	0

During the heating measurement period, the heat pump thermostats were programmed to hold weekly schedules where the ducted and ductless heat pumps would alternate in operation. For example, starting on November 11, ductless heat pumps operated Thursday 5:00 pm to Monday 5:00 pm (four days) and ducted heat pumps operated Monday 5:00 pm to Thursday 5:00 pm (three days). On December 20, the schedules were flipped, so ducted heat pumps operated Monday 5:00 pm to Friday 5:00 pm (four days) and ductless heat pumps operated Friday 5:00 pm to Monday 5:00 pm³¹.

Critical events during the heating tests are noted below:

- The House 3 native furnace shut off due to a malfunction on December 10 but was not observed until December 21. Repairs to the furnace fan were reportedly completed by the mobile home park maintenance staff on December 28; however, adjustments were inadvertently made to the native furnace thermostat that set the fan operation to “auto” (only turns on during heating). The furnace fan operation was not changed to “on” (runs at low speed continuously) until February 3. This significantly affected the air distribution of the ducted heat pump throughout the house, as we were depending on the furnace fan to circulate the ducted heat pump air through the native ductwork. The ductless heat pump was less affected by the furnace fan operation because its discharge air entered the main living space and was mixed by circulation fans.
- There were a few days where, due to a thermostat scheduling error, the System E ductless heat pump operated simultaneously with the System B ducted heat pump.
- A cold snap on December 22 and 23 froze water in the House 2 water pipes, causing a rupture at one or more locations³². Field staff were unable to visit the houses to turn water mains off and open faucets before the freeze occurred. When temperatures rose and water thawed, water leaked from the pipes into the floor assembly of the house, soaking the insulation and framing. The underbelly plastic was eventually pierced to allow water to drain and the insulation and framing to dry. The extent of leakage

³¹ Since the heating switchovers were at 5 PM, the heating “day” for each date in the data collection log is 5 PM the previous day to 5 PM

³² The cold snap also resulted in us turning on both heat pumps in house 3 (with the furnace not operating) for a few days to help prevent freezing



is still unknown—the mobile park leasing office will report to DNV repairs costs associated with the rupture. Figure 2-55 shows the relative amount of water that leaked into the underbelly. There is no evidence that the other houses had pipe ruptures.

All documented events are detailed in the data collection summary in APPENDIX A.

Figure 2-55. House 2 underbelly water leak due to pipe freeze and rupture



2.6 Heat pump decommissioning

On March 1, 2023, HP testing ended and disassembly and decommissioning of the HP systems and the instrumentation started.

Critical measurements were verified, and careful consideration was taken to safely pack and ship the HP equipment. The notable verifications before complete breakdown and disassembly included:

- Measure pressure drop on ducted units
 - Labor saver inlet to room
 - Room to duct box interior
 - Room to gap between labor savor and air handler
- Refrigerant line measurements
 - Total length of liquid and vapor lines to relevant points (bends, valves, etc.)
 - Relative position of sensors (MF sensor, pressure sensors) in line sets
- Elevation between indoor unit and outdoor unit
- Weight of refrigerant removed during draw down
- Verify sensor ID and locations; relative positioning (e.g., one to five, left to right) for air inlet and outlet sensor arrays



Table 2-23 documents the HP factory charges and the refrigerant charge recovered after draw down.

Table 2-23. Heat pump post-testing draw down refrigerant weights

System ID	Factory charge, lb of R-410A	Recovered charge
D	3.53	3.26
A	13.00	12.07
B	11.00	9.03**
E	4.08	3.77
F	3.70	3.25
C	3.75	3.00

** A pressure sensor on the vapor piping was dislodged just prior to the recovery process causing a refrigerant leak. An undetermined amount of refrigerant was vented to the atmosphere.

External static pressure measurements were taken at the inlet and discharge relative to the room. The figures below demonstrate the relative position of the probe locations. Note the filter slot was closed during the pressure tests.

Table 2-24. Differential pressure, inlet & discharge

System	Setting	Diff. pressure to room (Pa)	
		Inlet	Discharge
A	Low	91	-18.9
	Med	107.9	-24.2
	High	201	-45.6
B	Low	18.4	-5.6
	Med	181	-68.3
	High	281	-103.9
C	Low	57.4	-21.8
	Med	83.8	-31.5
	High	114.3	-42.7

Figure 2-56. Probe location for inlet and discharge, system A



Figure 2-57. Probe location for inlet, system A





2.7 Data dashboard

DNV produced a data dashboard building on an existing DNV data platform, LRS (<https://lrs.dnv.com/>). The platform was originally designed to handle advanced load research and statistical analysis. Data ingestion routines needed to be developed to accept the data collection devices used in this study. The data acquisition devices (eGauge, Onset) either pushed their interval data automatically or LRS queried the data logger using API calls to receive interval data.

Each house had cable internet, and all interval data was successfully transferred using the internet service. The “raw” register data are in 1-minute intervals for all variables/sensors. “Profiles” for each variable/sensor were developed so that the data could be visually charted and inspected in the dashboard. The profiles average the 1-minute data into 15-minute intervals to improve data loading and processing efficiency.

The data dashboard and remote connection to the data acquisition devices allowed DNV to actively monitor the over 300 data points and to receive notifications of failed sensors or failed data transfers. The remote monitoring allowed DNV to identify “drift” in the ducted HP differential pressure sensors, where the “zero” reading (when the indoor fan was off) drifted from 0 Pascals. DNV worked with UNL staff to troubleshoot the issue and eventually replace the faulty sensor. Remote monitoring also allowed DNV to verify that heat pump schedules were programmed correctly and alert us (indirectly) of malfunctions or unexpected operations.

There were, however, instances where alerts could have been programmed to communicate events that in retrospect were critical to testing conditions. For example, the native furnace fan operation was an important component for the testing conditions. It was not actively monitored using an automated alert feature, so its operation was only observed manually (via a team member visually identifying on the dashboard or in the field).

DNV produced monthly reports in the form of “data collection summaries” on data collection activities that summarized data collection issues that arose during the preceding month, and what was done to address the issues.

2.7.1 Direct measurements

Direct measurements are data that are collected via instrumentation in the houses. All direct measurements were delivered in one-minute intervals and most had one-second sampling³³. There were over 300 direct measurements collected during the testing period. It appears most sensors remained stable with only one known outright failure. The differential pressure sensor measuring effective air flow rate for System B was confirmed failed in early October and replaced October 25, 2022.

Most sensors appear to have measured accurate and confident readings, although decommissioning did not afford the opportunity to check the sensors’ measurements to a known calibrated value. Confidence in the

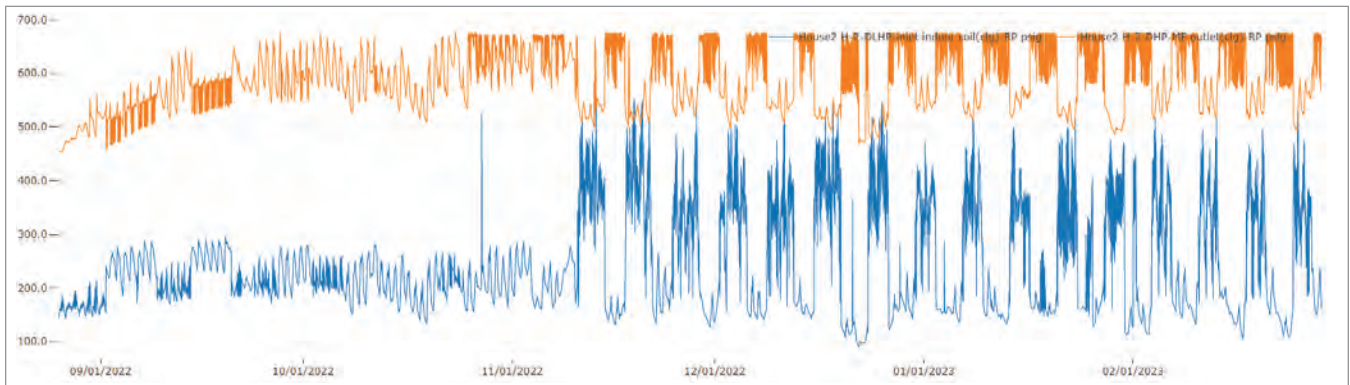
³³ The condensate sensors are state sensors that counted bucket tips. Its sampling was 1 minute. Certain weather station sensors could have had sampling greater than 1-second.

measurements is afforded through the comparison of like sensors measuring the same event. For example, nine different sensors measure the temperature of the ductless heat pump discharge/outlet air. When the system is off, all nine temperature sensors converge to the same temperature, within the reported accuracy range of the sensors. Positioning and placement of the sensors had some influence on their measurements as discussed above, but these were distinct from sensor failure.

There were some specific findings regarding sensor measurement quality and/or confidence:

- The gauge pressure sensors (installed to measure refrigerant pressure) are rated at 500 psig (with a 0-5 VDC analog output) and 0.9 percent full scale accuracy. Some of the specified operating pressures of the heat pumps exceeded 500 psig and there appear to have been instances where the pressure did exceed that value. During these moments, the accuracy of the sensor could be reduced.
- One of the gauge pressure sensors (System B mass flow outlet pressure) appears to have significantly drifted almost immediately after start-up. The data can almost certainly be discarded. The two sensors in Figure 2-58 should have the same pressure readings because they are essentially measuring the same point in the line set (across the mass flow sensor). The orange line is the drifted sensor and does not follow expected behavior. The sensor was not replaced because replacement would have potentially released refrigerant and given chance for leakage.

Figure 2-58. System B pressure gauge drift



- The differential pressure sensors (measuring ducted system air flow) installed on Systems A, B, and C all experienced start-up drift, where the zero-pressure point drifted such that the sensor would read nonzero pressure when the fans were off. The sensors have an “auto-zero” button to reset the sensor. This button had to be pressed multiple times during the initial start-up days. The sensor was considered stable after the measurements were observed to stay consistent with measurements made with a hand-held digital manometer (DG-700). However, the System B sensor appeared compromised, and it was eventually replaced.
- The CT used to measure the native furnace air handler was purposefully sized smaller (rated 5A) than the maximum current draw of the circuit. The intent was to accurately measure the fan power (rated 3.6A



maximum). However, the circuit also feeds the electric strip heat. When the electric strip heat turned on, the current was outside the rated range of the CT and the reading proved inaccurate.

- The System E mass flow sensor appears that it may have needed calibration offset. During periods of nonoperation the mass flow sensor measured nonzero values. The data may be corrected by applying a fixed offset.
- The temperature and relative humidity sensors (both RTD and thermocouple) all appear to have maintained their relative accuracies and did not experience noticeable drift. There were moments where the sensor was disconnected from the data logger (e.g., when System D IDU was replaced) and reported nonsensical data, but once re-connected, the sensor returned to expected operation.

2.7.2 Calculated measurements

“Dashboard equation” variables are calculated by defining direct measurements (e.g., outlet temperatures, power measurements) as input variables in equations. The following rules/assumptions were implemented into the dashboard equation variables:

- Currently, all sensors mapped to a particular variable (e.g., System A outlet air temperature) are averaged together to represent the variable value. There is ongoing discussion with the advisory committee to potentially exclude and/or weight some sensors. For example, there are nine sensors measuring ductless heat pump outlet air temperature; their measurements can vary significantly (by up to 20°C, when the unit is actively heating/cooling) based on positioning in the air stream. These nine sensors are all weighted equally when averaging together to represent the outlet air temperature used to calculate sensible capacity.
- Calculations are performed on the one-minute interval data. Hysteresis, response times, and other conditions can impact one-minute data such that data streams may not “line up” well at such a fine resolution. The intent is to provide as raw a calculated value as possible that can later be combined into more reasonable averages.
- There are no filters applied when performing the calculations. Data “noise” can cause unrealistic values to be calculated. For example, it might be known that System A is off during period X and therefore its total capacity and COP should be zero during period X. However, small differences in coil measurements, and signal noise in power and air flow measurements, can lead to sometimes significant values being calculated for capacity and COP. Post-analysis is expected to account for and filter out these conditions and accommodate appropriately.

Sections 2.7.2.1 to 2.7.2.6 define the calculated equations, their inputs, and the variable referencing to direct measurements.



2.7.2.1 Definitions and nomenclature

The heat pumps are labeled A through F. Three are ducted and three are ductless. Some of the equations are different for ducted and ductless heat pumps. The types are indicated in Table 2-25:

Table 2-25. Types of heat pumps

Type	House #	Pseudonym
Ducted	1	Heat Pump A
	2	Heat Pump B
	3	Heat Pump C
Ductless	1	Heat Pump D
	2	Heat Pump E
	3	Heat Pump F

DHP: ducted heat pump

- DLHP: ductless heat pump
- UOM: unit of measurement
- Outlet air: supply/discharge air downstream of the indoor air coil
- Inlet air: return air upstream of the indoor air coil
- Lower case q refers to airflow or liquid flow and upper-case Q refers to energy.
- “Inferred” means the calculated value derives from a fan power profile instead of a “measured” air flow rate. All ductless heat pump systems only have an “inferred” air flow rate. Thus, ductless system capacities are all “inferred,” despite the word “inferred” not being in the display name of the ductless system capacities calculations

Dry air density:

$$\rho_s = \frac{p_a}{R \times T_{s,abs}}$$

$$\rho_r = \frac{p_a}{R \times T_{r,abs}}$$

Where,

R is the specific gas constant for dry air; 287.051 [J / kg / K] [12]

$T_{r,K}$ is the temperature of the DHP or DLHP inlet air in degrees K [13]

$T_{s,K}$ is the temperature of the DHP or DLHP outlet air in degrees K [14]

p_a is the absolute pressure in Pa [9]



Humidity Ratio

The calculation registers use psychrometric programming packages to calculate humidity ratios (mass of water vapor in humid air to the mass of dry air) using:

- For humidity ratio of outlet air, use
 - Outlet air temperature (°C) [3]
 - relative humidity (%RH) of outlet air [26]
 - and p_a , the absolute pressure of ambient air, in Pa [9]
- For humidity ratio of inlet air, use
 - temperature (°C) [4]
 - relative humidity (%RH) of inlet air [27]
 - and p_a , the absolute pressure of ambient air, in Pa [9]

Inferred Airflow:

The calculated registers are named:

- H-3-DLHP-inferred-airflow
- H-3-DHP-inferred-airflow
- H-2-DLHP-inferred-airflow
- H-2-DHP-inferred-airflow
- H-1-DLHP-inferred-airflow
- H-1-DHP-inferred-airflow

We have developed an empirical relationship between fan power and airflow for all the HVAC systems. We also measured the airflow directly on the ducted HVAC units (systems HVAC A, HVAC B, and HVAC C).

For all heat pumps (systems A through F) we have an empirical relationship between fan power and airflow. The inferred airflow will be used for all capacity and COP calculations.

$$q_{fan} = \left(\frac{Q_f - C}{A} \right)^{\frac{1}{3}}$$

$$q = 0.00047194745 \times q_{fan}$$

Where,

Q_f is the measured fan power of the heat pump [W]³⁴

q_{fan} is the inferred airflow of the heat pump [ft³ / min] [48]

q is the airflow in [m³ / s] [5]

A and C are empirically determined coefficients (see table below).

³⁴ Note that these measured values are technically the measured power of the indoor units which include the fan power, transformer losses, control electronics, thermostat, etc.



Table 2-26. Values of A and C by system

System	Type	Qf variable number	Value of A	Value of C
HVAC A	Ducted	[42]	6.86E-07	22.4
HVAC B	Ducted	[44]	5.44E-07	9.65
HVAC C	Ducted	[46]	7.10E-07	4.16
HVAC D	Ductless	[43]	1.81E-07	8.52
HVAC E	Ductless	[45]	1.43E-07	6.46
HVAC F	Ductless	[47]	5.20E-07	4.81

Measured Airflow:

The calculated registers are named:

- H-3-DHP-measured-airflow
- H-2-DHP-measured-airflow
- H-1-DHP-measured-airflow

For DHP the volumetric airflow, q_{DHP} [49], must be converted from $q_{DHP,s}$ [15]. [15] is the “raw” measured value from LRS and assumes standard conditions and its UOM is m^3/s .

The measured airflow [15] assumes “standard” conditions i.e., assumes the following:

$$\sqrt{\frac{NSOP}{TFSOP}} = 1$$

$$\rho_f = 1$$

To convert [15] to [49]:

$$q_{DHP} = \sqrt{\frac{1.2014}{\rho_r}} \times q_{DHP,s}$$

Where,

ρ_r is the dry air density of inlet air [2]

q_{DHP} is the volumetric “measured” airflow [49]

$q_{DHP,s}$ is the indicated (assumed atmospheric air density of $1.204 \text{ kg}/m^3$) air flow rate in m^3 / s [15]. This is the value that LRS produces. The Python code must transform this variable [15] to the volumetric air flow rate [49]

$q_{DHP,s}$ is the indicated (assumed atmospheric air density of $1.204 \text{ kg}/m^3$) air flow rate in m^3 / s [15]. This is the value that LRS produces. The Python code transforms this variable [15] to the volumetric air flow rate [49]



HVAC System Power

The total input power Q_i of the heat pump is calculated differently depending on the HVAC system. **Note that the sensor data queried from LRS will be in Watts**

- Q_i (HVAC A) = Outdoor unit power [kW] [19] + Indoor unit power [kW] [42]
- Q_i (HVAC B) = Indoor unit power [kW] [21] + Outdoor unit power [kW] [22]
- Q_i (HVAC C) = Total input power [kW] [24]
- Q_i (HVAC D) = Total input power [kW] [20]
- Q_i (HVAC E) = Total input power [kW] [23]
- Q_i (HVAC F) = Total input power [kW] [25]

Table 2-27. Table of variables

Variable Number [##]	Variable symbol	Variable name	Variable units	Notes
1	ρ_s	Dry air density of outlet air	kg / m ³	See 2.7.2.1
2	ρ_r	Dry air density of inlet air	kg / m ³	See 2.7.2.1
3	T_s	Dry bulb temperature of outlet air	°C	
4	T_r	Dry bulb temperature of inlet air	°C	
5	q	Inferred Inlet air flow	m ³ / s	See 2.7.2.1 This variable is a product of converting [48] from IP to SI units
6	C_p	Specific heat capacity of air	kJ / kg / °C	Constant value equal to 1.006
7	W_s	Humidity ratio of outlet air	unitless (kg water / kg dry air)	See 2.7.2.1
8	W_r	Humidity ratio of inlet air	unitless (kg water / kg dry air)	See 2.7.2.1
9	p_a	Absolute pressure of ambient air	Pa	Convert mbar to Pa by multiplying mbar by 100
10	h_s	Enthalpy of outlet air	kJ / kg	
11	h_r	Enthalpy of inlet air	kJ / kg	
12	R	Specific gas constant for dry air	J / kg / K	Constant value equal to 287.051
13	$T_{r,K}$	Dry bulb temperature of inlet air	K	Calculate by converting [4] to K
14	$T_{s,K}$	Dry bulb temperature of outlet air	K	Calculate by converting [3] to K
15	q_{DHP_s}	True flow plate flow used for DHP airflow measurements. This variable assumes standard air density of 1.204 kg/m ³ . See 49 for volumetric flow value	m ³ /s	This variable is a prerequisite for producing variable [49]
16	$T_{r,F}$	Dry bulb temperature of DHP inlet air	°F	Calculate by converting [4] to °F
17	ρ_f	Air density factor	unitless	See 2.7.2.1
18	Q_i	Total input power of the heat pump	kW	See 2.7.2.1



19		HVAC A outdoor unit power	kW	See 2.7.2.1. Note that sensor data UOM is Watts. It must be converted to kW by dividing by 1000
20		HVAC D total input power	kW	See 2.7.2.1. Note that sensor data UOM is Watts. It must be converted to kW by dividing by 1000
21		HVAC B indoor unit power	kW	See 2.7.2.1. Note that sensor data UOM is Watts. It must be converted to kW by dividing by 1000
22		HVAC B outdoor unit power	kW	See 2.7.2.1. Note that sensor data UOM is Watts. It must be converted to kW by dividing by 1000
23		HVAC E total input power	kW	See 2.7.2.1. Note that sensor data UOM is Watts. It must be converted to kW by dividing by 1000
24		HVAC C total input power	kW	See 2.7.2.1. Note that sensor data UOM is Watts. It must be converted to kW by dividing by 1000
25		HVAC F total input power	kW	See 2.7.2.1. Note that sensor data UOM is Watts. It must be converted to kW by dividing by 1000
26		Relative humidity of outlet air	RH%	See 2.7.2.1
27		Relative humidity of inlet air	RH%	See 2.7.2.1
28	q_w	Volume flow rate of condensate	m^3 / s	See 2.7.2.4. Sensor data one-minute values in mL (per minute). Convert to m^3 / s by dividing one-minute values by 60 s / min (and converting mL to m^3)
29		Mass flow rate of refrigerant	kg / s	Sensor data in g / s. Must convert to kg / s
42	Q_{fA}	HVAC A indoor unit power	kW	See 2.7.2.1. Note that sensor data UOM is Watts. It must be converted to kW by dividing by 1000
43	Q_{fB}	HVAC D indoor unit power	kW	See 2.7.2.1. Note that sensor data UOM is Watts. It must be converted to kW by dividing by 1000
44	Q_{fC}	HVAC B indoor unit power	kW	See 2.7.2.1. Note that sensor data UOM is Watts. It must be converted to kW by dividing by 1000
45	Q_{fD}	HVAC E indoor unit power	kW	See 2.7.2.1. Note that sensor data UOM is Watts. It must be converted to kW by dividing by 1000
46	Q_{fE}	HVAC C indoor unit power	kW	See 2.7.2.1. Note that sensor data UOM is Watts. It must be converted to kW by dividing by 1000
47	Q_{fF}	HVAC F indoor unit power	kW	See 2.7.2.1. Note that sensor data UOM is Watts. It must be converted to kW by dividing by 1000
48	q_{fan}	HVAC airflow inferred from fan power	$ft^3 / minute$	See 2.7.2.1
49	q_{DHP}	True flow plate flow used for DHP airflow measurements. This variable is corrected for actual air density.	m^3/s	This variable is a product from converting [15] from standard conditions to actual conditions
50	T_{out}	Outdoor air temperature	$^{\circ}C$	



2.7.2.2 Indoor air enthalpy method: sensible capacity

There are two “versions” of air side sensible capacity. One version uses “measured” airflow [49] and **applies to DHP systems only**. (HVAC A, B, and C). The second version uses “inferred” airflow [5] and **applies to all HVAC systems**

$$\text{Sensible Capacity: } Q_s[kW] = |T_s - T_r| \times \rho_r \times q_{DHP} \times C_p$$

Where:

ρ_r is the dry air density of the DHP or DLHP inlet air [kg / m3] (measured temperature relationship to density of dry air). See 2.7.2.1 [2]

T_s is the temperature of the outlet air [°C] (average of the outlet air sensors) [3]

T_r is the temperature of the inlet air [°C] (average of the return air sensors) [4]

q_{DHP} is the airflow [m3 / s] (measured by TruFlow for ducted). See 2.7.2.1. [49]

C_p is 1.006 [kJ / kg / °C], the specific heat capacity of air at 0 °C and 1 bar [6]

The calculated registers are named:

- H-3-DHP-Air side sensible-capacity
- H-2-DHP-Air side sensible-capacity
- H-1-DHP-Air side sensible-capacity

$$\text{Inferred Sensible Capacity: } Q_s[kW] = |T_s - T_r| \times \rho_r \times q \times C_p$$

Where:

ρ_r is the dry air density of the DHP or DLHP inlet air [kg / m3] (measured temperature relationship to density of dry air). See 2.7.2.1 [2]

T_s is the temperature of the outlet air [°C] (average of the outlet air sensors) [3]

T_r is the temperature of the inlet air [°C] (average of the return air sensors) [4]

q is the airflow [m3 / s] (inferred from power/flow relationships). See 2.7.2.1. [5]

C_p is 1.006 [kJ / kg / °C], the specific heat capacity of air at 0 °C and 1 bar [6]

The calculated registers are named:

- H-3-DHP-inferred air side sensible-capacity
- H-2-DHP-inferred air side sensible-capacity
- H-1-DHP-inferred air side sensible-capacity
- H-3-DLHP-Air side sensible-capacity
- H-2-DLHP-Air side sensible-capacity
- H-1-DLHP-Air side sensible-capacity

The DLHPs don’t have the word “inferred” because there is only one sensible capacity calculated for DLHPs.



2.7.2.3 Indoor air enthalpy method: latent capacity

There are two “versions” of air side latent capacity. One version uses “measured” airflow [49] and **applies to DHP systems only**. (HVAC A, B, and C). The second version uses “inferred” airflow [5] and **applies to all HVAC systems**.

Latent Capacity: $Q_l[kW] = |W_s - W_r| \times \rho_r \times q_{DHP} \times h_{we}$

And the latent heat vaporization of water: $h_{we}[kJ/kg] = 2494 - 2.2(T_s)$

Where:

ρ_r is the density of the DHP or DLHP inlet air [kg / m³] (measured temperature relationship to density of dry air) [2]

W_s is the humidity ratio in the outlet air [kg water / kg dry air] (average of the outlet air sensors). See 2.7.2.1 [7]

W_r is the humidity ratio in the inlet air [kg water / kg dry air] (average of the inlet air sensors). See 2.7.2.1 [8]

q_{DHP} is the airflow [m³ / s] (measured by TruFlow for ducted). See 2.7.2.1 [49]

T_s is the temperature of the outlet air (average of outlet air sensors) [°C] [3]

The calculated registers are named:

- H-3-DHP-Air side latent-capacity
- H-2-DHP-Air side latent-capacity
- H-1-DHP-Air side latent-capacity

Inferred Latent Capacity: $Q_l[kW] = |W_s - W_r| \times \rho_r \times q \times h_{we}$

And the latent heat vaporization of water: $h_{we}[kJ/kg] = 2494 - 2.2(T_s)$

Where:

ρ_r is the density of the DHP or DLHP inlet air [kg / m³] (measured temperature relationship to density of dry air) [2]

W_s is the humidity ratio in the outlet air [kg water / kg dry air] (average of the outlet air sensors). See 2.7.2.1 [7]

W_r is the humidity ratio in the return air [kg water / kg dry air] (average of the inlet air sensors). See 2.7.2.1 [8]

q is the airflow [m³ / s] (inferred from power/flow relationships). See 2.7.2.1 [5]

T_s is the temperature of the outlet air (average of outlet air sensors) [°C] [3]

Note: in heating mode, the latent capacity is zero; however, the calculated variable is not programmed to determine operating mode. As a result, latent capacities are calculated in heating mode due to small differences in the measured inlet and outlet humidity ratios.

The calculated registers are named:

- H-3-DLHP-Air side latent-capacity
- H-2-DLHP-Air side latent-capacity
- H-1-DLHP-Air side latent-capacity
- H-3-DHP-inferred air side latent-capacity



- H-2-DHP-inferred air side latent-capacity
- H-1-DHP-inferred air side latent-capacity

2.7.2.4 Condensate-measured latent capacity

We will have condensate flow in mL in one-minute intervals. At the one-minute interval, the unit is mL but can be seen as a condensate volumetric flow rate of mL/min. When the one-minute values are combined to 15-minute averages the UOM is mL/min.

$$\text{Latent Capacity: } Q_{l,w}[kW] = h_{we} \times \rho_w \times q_w$$

$$\text{And the latent heat vaporization of water: } h_{we}[kJ/kg] = 2494 - 2.2(T_s)$$

Where:

ρ_w is the density of water, approximately 997 [kg / m3]

q_w is the volume flow rate of condensate (measured by the rain gauge) [m3 / s] [28]

T_s is the temperature of the outlet air (average of outlet sensors) [°C] [3]

The calculated registers are named:

- H-3-DLHP-Condensate latent-capacity
- H-3-DHP-Condensate latent-capacity
- H-2-DLHP-Condensate latent-capacity
- H-2-DHP-Condensate latent-capacity
- H-1-DLHP-Condensate latent-capacity
- H-1-DHP-Condensate latent-capacity

2.7.2.5 Indoor air enthalpy method: total capacity

There are two “versions” of air side total capacity. One version uses “measured” airflow [49] and **applies to DHP systems only**. (HVAC A, B, and C). The second version uses “inferred” airflow [5] and **applies to all HVAC systems**

$$\text{Total Capacity: } Q_t[kW] = |h_s - h_r| \times \rho_r \times q_{DHP}$$

Where:

ρ_r is the density of the inlet air [kg / m3] (measured temperature relationship to density of dry air) [2]

h_s is the enthalpy of the outlet air [kJ / kg] (average of the outlet RH sensors) [10]

h_r is the enthalpy of the inlet air [kJ / kg] (average of the return RH sensors) [11]

q_{DHP} is the airflow [m3 / s] (measured by TruFlow for ducted) [49]



The calculated registers are named:

- H-3-DHP-Air side total-capacity
- H-2-DHP-Air side total-capacity
- H-1-DHP-Air side total-capacity

Inferred Total Capacity: $Q_t [kW] = |h_s - h_r| \times \rho_r \times q$

Where:

ρ_r is the density of the inlet air [kg / m³] (measured temperature relationship to density of dry air) [2]

h_s is the enthalpy of the outlet air [kJ / kg] (average of the outlet RH sensors) [10]

h_r is the enthalpy of the inlet air [kJ / kg] (average of the return RH sensors) [11]

q is the airflow [m³ / s] (inferred from power/flow relationships) [5]

Note: in heating mode the total capacity should equal the sensible capacity (latent capacity is zero); however, the calculated registers are not programmed to assign “0” to latent capacity while the systems are in heating mode. Thus, small differences in sensors readings can lead to nonzero latent capacities.

The calculated registers are named:

- H-3-DLHP-Air side total-capacity
- H-2-DLHP-Air side total-capacity
- H-1-DLHP-Air side total-capacity
- H-3-DHP-inferred air side total-capacity
- H-2-DHP-inferred air side total-capacity
- H-1-DHP-inferred air side total-capacity

2.7.2.6 Coefficient of performance (COP)

There are two “versions” of COP. One version uses “measured” airflow [49] and **applies to DHP systems only**. (HVAC A, B, and C). The second version uses “inferred” airflow [5] and **applies to all HVAC systems**. Note that COP values are provided for reference, and that one-minute, 15-minute or even hourly COPs can be of limited use because of transient conditions. Typically more granular data of capacity and power input can be integrated over longer time periods of interest to obtain useful COP values.

COP [“measured” applies to HVAC A, B, and C and “inferred” applies to all]:

$$COP = \frac{Q_t}{Q_i}$$

Where,

Q_t is the total capacity [inferred or measured] [kW]

Q_i is the total input power of the heat pump indoor unit and outdoor unit [kW] [18]



The calculated registers are named:

- H-3-DLHP-Air side-FCOP
- H-3-DHP-Air side-FCOP
- H-2-DLHP-Air side-FCOP
- H-2-DHP-Air side-FCOP
- H-1-DLHP-Air side-FCOP
- H-1-DHP-Air side-FCOP
- H-3-DHP-inferred air side-FCOP
- H-2-DHP-inferred air side-FCOP
- H-1-DHP-inferred air side-FCOP



PHASE 2: (LAB TESTING) AND NEXT STEPS

As part of Phase 1 data collection and analysis, the direct measurements and calculated measurements for each heat pump are presented in the data dashboard (as 15-minute profiles). All direct and calculated measurements are provided in tab-separated files of one-minute data.

The Phase 1 analysis plan stated a list of desired study results and measurements that were proposed to be available on the data dashboard. The following features were successfully implemented:

- Indoor Air Enthalpy Method Capacity: sensible, latent, and total capacities; and instantaneous COP
- Power usage for indoor and outdoor heat pump units and whole house
- Supplementary data such as indoor and outdoor dry and wet-bulb temperature, refrigerant temperature and pressure, refrigerant mass flow rate, etc.

The dashboard shows all heat pump testing historic data and while the heat pump testing period was ongoing, showed direct data as recent as one hour. The dashboard allows the user to view historic values in 15-minute profiles, by system and house.

Additional analysis tasks have been extended into the Phase 2 budget and timeline. The FSCOP_c, FSCOP_h values will be calculated using the bin hours from Region IV per Appendix M1 and using the bin hours listed in CSA SPE-07. In the final Phase 2 report, after the laboratory tests are completed, the DNV team, in collaboration with the Technical Advisory Committee, will compare the CSA SPE-07 and Appendix M1 SEER₂, HSPF₂, SCOP_c, and SCOP_h to the field-measured FSCOP_c and FSCOP_h. The field performance will be compared on a normalized basis to the test laboratory field performance (e.g., percent deviation from HSPF₂ and percent deviation from SCOP_h). Daily COP vs. daily outdoor air temperature values from the field measured tests will be plotted and analyzed. Other Phase 2 analysis goals are:

- To determine the characteristics that might be factored into heat pump efficiency metrics or enhance test procedures, DNV proposes to study suspected characteristics or conditions that might affect field operation relative to laboratory operation. These include:
- The relationship between turn-down ratio and other part-load performance attributes and heat pump heating performance
- Instances with particularly low turn-down
- Instances where there is significant cycling
- Cycling penalties at part load conditions
- Compressor speed modulation between milder and more extreme outdoor temperatures
- Patterns around defrost energy use, crank-case heater use, and standby power use
- Specific outdoor temperatures, such as low heating temperatures (5°F), mild heating temperatures (47°F), mild cooling temperatures (82°F), and high cooling temperatures (95°F)

Upon completion of Phase 2 testing, DNV will produce a file that compares published nameplate ratings, laboratory-produced Appendix M2 SEER₂ and HSPF₂ ratings, field-tested FSCOP_c and FSCOP_h, and laboratory-



produced CSA SPE-07 SCOPC and SCOPH ratings. The comparisons will include measurement uncertainty propagated in accordance with established principles.

Phase 2 lab testing is planned to continue through the second week of July 2023 with phase 2 analysis tasks slated for completion by the second week of September. Phase 2 reporting will continue through September with a final reporting date in October 2023.





